Tutor/s

Dra. Anna Maria Costa
Departament de Química Inorgànica i Orgànica

Dr. José Luis Abad
RUBAM-IQAC-CSIC

Grau de Química

Treball Final de Grau

Synthesis of phytosphingosine and phytoceramide probes to study the sphingolipid metabolism in non-alcoholic fatty liver disease.

Síntesis de sondas de fitoesfingosina y fitoceramida para estudiar el metabolismo de los esfingolípidos en la enfermedad del hígado graso no alcohólico.

Marina Casas Acero

June 2021

Universitat de Barcelona

B:KC Barcelona Knowledge Campus
Campus d'Excel·lència Internacional

A mis docentes, quien me guiaron en el proceso de obtención de mi título universitario, y en especial a mi tutor por su ayuda, paciencia y dedicación. Sus conocimientos me han ayudado a reforzar mi aprendizaje.

REPORT

CONTENTS

1. SUMMARY

Evidence demonstrates that downregulation of DES1 activity, altering dihydroceramides ratio, is involved in the primordial causes of non-alcoholic fatty liver disease (NAFLD). Although DES2 and regulation of phytoceramides are also considered to be involved in the development of this disease, not enough studies exist to prove it.

This work has essentially developed and evaluated a synthetic procedure capable of providing both non-natural C17 phytosphingosine and phytoceramide probes with D-*ribo*-stereochemistry to be used in the study of the stated problem through its administration in mice for HRMS-HPLC monitorization. Some of the probes are commercially available but economically inaccessible for the amounts needed to perform animal assays. Target compounds were characterized by stereochemical control of the dihydroxylation intermediates from their specific optical rotation, NMR analysis and MS. Additionally, the natural C18 phytoceramide was prepared as a reference standard from a commercially available phytosphingosine.

Keywords: NAFLD, metabolism, DES1, DES2, sphingolipid, sphingoid base, phytosphingosine, ceramide, phytoceramide, probes, D-*ribo*-stereochemistry, Garner's aldehyde, Wittig reaction, *syn*-dihydroxylation.

2. RESUMEN

La evidencia demuestra que la alteración de la actividad de la DES1 está implicada en las causas primordiales de la enfermedad no-alcohólica del hígado graso (ENAHG), alterando la proporción de dihidroceramidas. Aunque también se considera que la DES2 y la regulación de las fitoceramidas están implicadas en el desarrollo de esta enfermedad, no hay suficientes estudios que lo justifiquen.

En este trabajo se ha desarrollado y evaluado un procedimiento sintético capaz de proporcionar sondas no naturales de fitoesfingosina y fitoceramida C17 con D-*ribo*-estereoquímica para ser utilizadas en el estudio del problema planteado mediante su administración en ratones y monitorización por HRMS-HPLC. Algunas de las sondas son comercialmente asequibles, pero económicamente inaccesibles en las cantidades necesarias para la realización de los estudios biológicos propuestos. Los compuestos obtenidos se caracterizaron mediante el control estereoquímico de los intermedios de dihidroxilación a partir de su rotación óptica específica, análisis RMN y EM. Además, se preparó la fitoceramida natural C18 como estándar de referencia a partir de una fitoesfingosina comercial.

Palabras clave: EHGNA, metabolismo, DES1, DES2, esfingolípido, base esfingoide, fitoesfingosina, ceramida, fitoceramida, sonda, D-*ribo*-estereoquímica, aldehído de Garner, reacción de Wittig, dihidroxilación *syn*.

3. INTRODUCTION

Non-alcoholic fatty liver disease (NAFLD) involves a wide variety of pathologies such as hepatic steatosis, non-alcoholic steatohepatitis (NASH) and hepatocarcinoma. NAFLD has a multifactorial origin, and its principal cause is related to abnormal fat deposition in liver. Although triglycerides are strongly involved with this pathology, sphingolipids (SLs), and more concretely ceramides, seem to be associated with its development. An unbalanced ratio between ceramides and final metabolic products in the liver plasma induces weight gain, inflammation, and insulin resistance. In fact, ceramides may be biomarkers for NAFLD (Régnier et al., 2019).

3.1. SL METABOLISM

SLs are a complex class of bioactive lipids and are found in most organisms. Despite this, they exist in low abundance, less than 20% of the total mass of glycerophospholipids, which are the most common type found in the human body(Régnier et al., 2019).

SLs are classified into four subfamilies: phosphosphingolipids, glycosphingolipids, sphingoid bases and ceramides. They all share a common structure, which is made of a sphingoid base linked to a long-chain base through an amide bond. The acyl chain length of the fatty acid depends on the SL species. Distinction between the different SLs is based on the type of functional substituent at the C1-oxygen atom.

For ceramides, the substituent is an alcohol, for glycosphingolipids a sugar molecule (such as glucose, Fig. 1) and for phosphosphingolipids, a phosphate group. The single sphingoid bases (sphinganine, sphingosine or phytosphinosine) can also be found independently.

Sphingoid bases are relevant precursors for the SL metabolism. It has been seen that phytosphingosine has a wide variety of biological functions such as cell differentiation, signal transduction, regulation, proliferation and induction of apoptosis(Howell & Ndakala, 2005).

Among all eight stereoisomers of phytosphingosine, (*2S,3S,4R*)-2-aminooctadecane-1,3,4-triol with D-*ribo*-stereochemistry is the most common (Howell & Ndakala, 2005). D-*ribo*-phytosphingosine was first isolated in mushrooms and, thanks to its similarity to sphingosine, it

was named this way. Nowadays it is known that it also contributes as structural component in yeast, fungi, mammalian, and marine organisms.

The long chain of phytosphingosines is mainly made of 18 carbons, although a minor group of them have other chain lengths, specially C20 (Howell & Ndakala, 2005).

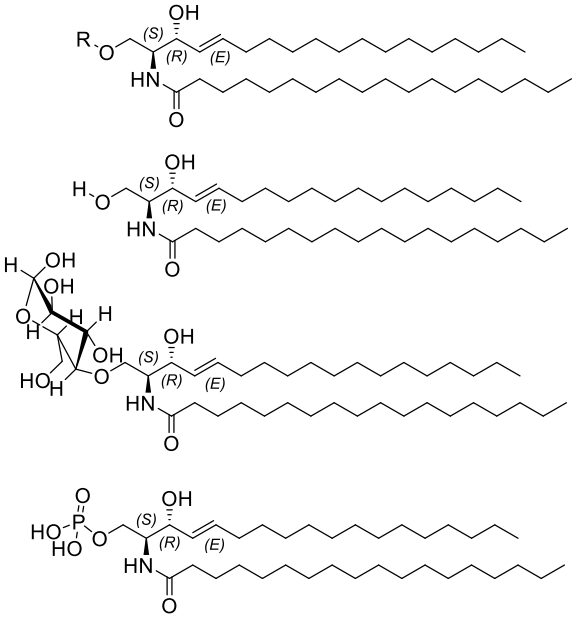

Figure 1. Different SL structures depending on the molecule attached to the C1-oxygen atom.

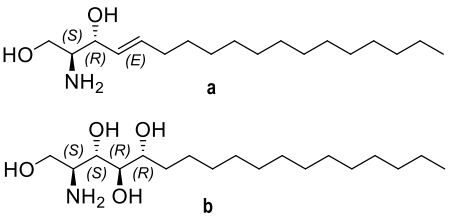

Figure 2. Differentiation between sphingoid bases**: 2a** corresponds to a sphingosine structure and **2b** to the phytosphingosine.

SLs seem to be related with the regulation of several biological processes. In fact, they are involved in different biological mechanisms, such as cell signaling, secretion and endocytosis. Besides, they are structural membrane components as well. Thus, they contribute to shape membranes and to arrange well-ordered domains. These arrangements are called lipid rafts (Régnier et al., 2019).

3.1.1. SL biosynthesis

De novo biosynthesis of SLs has its start in the endoplasmic reticulum (ER). The first step is the condensation of serine and palmitoyl-CoA thanks to the catalytic serine palmitoyl transferase (SPT). A ketone, 3-keto-sphinganine, is obtained, which is reduced by keto-sphinganine reductase (KSPR). As a result, sphinganine is obtained, and it is later acylated thanks to the ceramide synthases (CerSs). This forms a dihydroceramide, which is desaturated and generates a ceramide by the action of DES1 (Δ-4-dihydroceramide desaturase 1) (Régnier et al., 2019).

Several types of CerSs exist in the human body. The most common is CerS2, which synthetizes long chain ceramides and it is used mainly in the liver. For instance, long chain ceramides are predominant in healthy humans(Régnier et al., 2019).

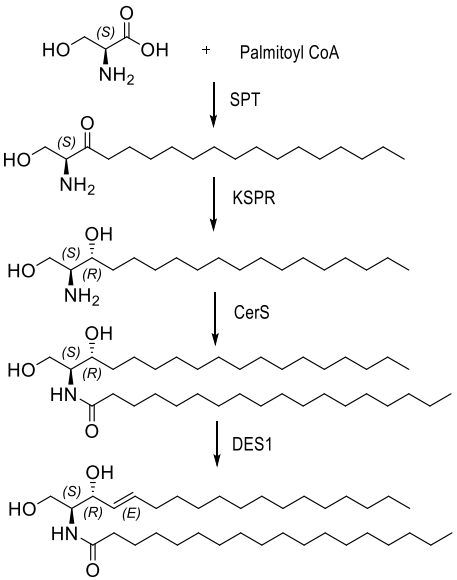

Figure 3. Sequence of reactions in the *de novo* biosynthesis of ceramide happening in the ER.

After the *de novo* synthesis in the ER, ceramides can be taken to the Golgi apparatus by vesicular transport, where they are transformed into sphingomyelin, glycosylated into glucosylceramides, or delivered by the ceramide transport protein. Afterwards, in the case of glucosylceramides and sphingomyelin, they are transported to the plasma membrane, also by vesicular transport (Régnier et al., 2019).

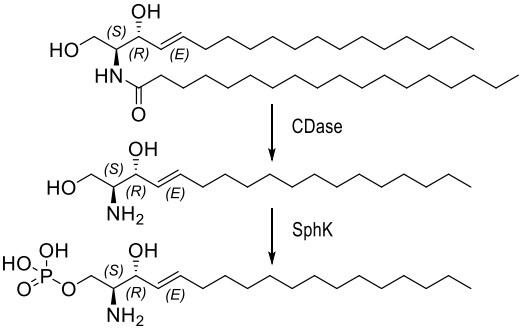

Figure 4. Sequence of reactions in the *de novo* biosynthesis of S1P happening in plasma membrane.

Once sphingomyelin is in the plasma membrane, it can be hydrolyzed to ceramide thanks to neutral or acid sphingomyelinase. Next, ceramide can be transformed by neutral ceramidase (CDase) into a bioactive signaling base (sphingosine), which can be finally phosphorylated into sphingosine-1-phosphate (S1P) by sphingosine kinases (SphKs) (Régnier et al., 2019).

In addition, sphingomyelin can be further internalized with glycosphingolipids into the endocytic vesicle to reach the lysosomal compartment, where it is hydrolyzed into ceramide, which is further hydrolyzed by CDase to form sphingosine. This sphingosine can be recycled in the ER into ceramide by the salvage pathway, which represents a major part of the total SL biosynthesis(Régnier et al., 2019).

3.1.2. Role of SLs in non-alcoholic fatty liver disease

NAFLD represents a worldwide chronic disorder and it has a prevalence of 3-6% in the population(Pagadala et al., 2012). The sickness gets developed in several stages.

The first one corresponds to hepatic steatosis, which implies the accumulation of triacylglycerides in hepatocytes due to an unbalanced proportion between the accumulation of these compounds in front of their expenditure. This is explained by an excessive population of these lipids in the liver cells membrane, excessive lipolysis, and deficit in fatty acid oxidation. This

stage may result reversible and unharmful, but unfortunately it can develop NASH, cirrhosis and hepatocellular carcinoma (Régnier et al., 2019). Further stages are characterized by steatosis, lobular and portal inflammation, apoptosis, cell death and fibrogenesis.

3.1.2.1. SLs as signaling factors in metabolic disorders

Liver is the main hub for SLs biosynthesis, highlighting sphingomyelin and ceramide. That is the reason why it implies a high level of toxicology referring to SLs. Other SLs are also critical to the development of NAFLD, such as dihydroceramides and sphingomyelin. Furthermore, this toxicology contributes to overweight, inflammation, insulin resistance and oxidative stress. These effects also take place in other organs (adipose tissue, musculoskeletal system, and heart, for example). The presence of a considerable quantity of saturated fatty acids such as palmitoyl may promote the synthesis of SLs, as they are biometabolical substrates used to produce them (by SPT and CerS enzymes). In addition to this, SLs and glycerolipids share several related metabolic pathways(Régnier et al., 2019).

It has been seen that in obesity, weight gain gets suppressed or slowed thanks to the attenuation in the action of several enzymes that take part in SL metabolism (SPT, CerS and SMS2) (Longato et al., 2012) and that the mRNA expression of neutral and acid sphingomyelinases (SMases) and, consequently, SLs content are higher in obese mice (Boini et al., 2010).

There exist two forms or main causes for the development of NAFLD and its further stage NASH. The first consists of liver degradation (due to obesity) to fatty liver, which is related to peripheral and hepatic insulin resistance. In steatosis, accumulation of hepatic triglyceride is caused by an increased calorie intake and *de novo* lipogenesis. Insulin resistance may promote this process by increasing free fatty acid delivery by adipose tissue lipolysis and by stimulation of anabolic processes by hyperinsulinemia(Régnier et al., 2019).

The second contemplates oxidative stress, hepatotoxicity (caused by free fatty acids, as explained before) hyperinsulinemia, increased intrahepatic cholesterol, and increased cytokines. This leads to inflammation and fibrosis by increasing lipid peroxidation due to several factors that contribute to oxidative stress (Régnier et al., 2019).

3.1.3. Dihydroceramide desaturases

As previously seen in section 3.1.1, the main source of ceramides is the *de novo* pathway, in which the final reaction corresponds to the synthesis of an olefin catalyzed by DES1 to add a 4,5-*trans*-double bond on the sphingoid base of the dihydroceramide. On the other hand, DES2, catalyzes the synthesis of phytoceramides, adding instead two alcohol functional groups in the mentioned carbons. Phytosphingosine occurrence has presence in skin, intestine, and kidney(Barbarroja et al., 2015).

There is evidence that down regulation of DES1 increases the relationship between dihydroceramides and ceramides in several cellular models, and there is as wide evidence for the first ones to be considered modulators of cell cycle, apoptosis, autophagy or oxidative stress, processes that commit the function and development of adipose tissue (Barbarroja et al., 2015).

As mentioned, several studies relate DES1 metabolism with the development of NAFLD into hepatic steatosis and NASH, but none of it considers the action of DES2. With these antecedents the main objective of the research is to synthetize potential biomarkers to study the relationship between this enzyme and the cited disorder. This work is specifically focused on the synthesis of a non-natural C17 phytosphingosine and the respective palmitoylated phytoceramide to be used as probes for the study of SL metabolism in mice liver. These probes with an odd number of carbons will be introduced in the organisms and the sequence of biological paths will be tracked by HRMS-HPLC. For these studies, a minimum quantity of 250 mg of the free sphingoid base and 500 mg of the phytoceramide are necessary.

3.2. SYNTHESIS OF C17-PHYTOSPHINGOSINE AND C17-PHYTOCERAMIDE PROBES

Natural ceramides usually contain a long chain with an even number of carbons in the sphingoid base (mostly C18 and upper). In this study, it has been decided to synthesize a C17 phytosphingosine base and its respective palmitoylated phytoceramide to control the DES2 metabolic activity. To do that, tracking of the metabolized tagged phytosphingosine probe and the use of a phytoceramide standard can help to differentiate the metabolism of SLs partners present in the organism. In addition, C17-phytoceramide metabolism can be further followed.

There are a number of articles in the literature describing the preparation of (phyto)ceramides using L-serine as raw material [(Azuma et al., 2000; Imashiro et al., 1998)]. In this work, the synthetic pathway starts from properly protected methyl ester coming from L-serine (an advanced

intermediate of one of those synthesis). Reduction to the Garner´s alcohol and its oxidation give rise to Garner´s aldehyde as key intermediate. From these references, the aim is to develop a synthetic procedure capable of producing truncated phytosphingosines and phytoceramides from other previously described synthesis[(Azuma et al., 2000; Imashiro et al., 1998)].

3.2.1. An alternative pathway to the synthesis of modified Jaspine B and its derivatives

The establishment of a synthetic procedure for the synthesis of phytoceramides will also serve as an entry point for the synthesis of jaspines (Abraham et al., 2008).

The synthesis of isomeric jaspines (anhydro phytosphingosines), arising from intramolecular cyclization of the corresponding phytosphingosines with different configurations at C3 and C4 positions of the sphingoid backbone was reported (Canals et al., 2009, p. 135). Natural jaspine B (pachastrissamine) is the most cytotoxic isomer on A549 cells and it induces cell death in a dose-dependent manner. The cytotoxicity of jaspine B has been correlated with a significant increase of intracellular dihydroceramides, which seem to play an active role in autophagy (Canals et al., 2009).

Although the synthesis of the latter compounds is not part of the objectives of the work, implementation of the synthetic pathway to the different stereoisomers of truncated phytosphingosines will be very useful for the synthesis of the different stereoisomers of modified Jaspines.

4. OBJECTIVES

Based on the previously discussed topics, the following objectives were considered:

1. Set up the conditions and synthesis of truncated phytosphingosines with D-*ribo*-stereochemistry and their respective palmitoylated phytoceramides.
2. Synthesis of corresponding mass tagged C17-phytosphingosine and phytoceramide.
3. Implementation of a pathway for the synthesis of truncated phytosphingosines as an entry route to the synthesis of modified Jaspines.

5. EXPERIMENTAL SECTION

5.1. MATERIALS AND METHODS

Most of the reagents were purchased from Sigma-Aldrich and Acros. Commercially available reagents were used with no further purification. All reactions were monitored by TLC analysis using MERCK® TLC Silicagel 60G F_{254}. UV light (265 nm) was used as visualizing agent and a 5% (w/v) solution of phosphomolybdic acid in ethanol was used as staining agent. Compounds were purified by flash column chromatography using Sigma-Aldrich silica gel (pore size 60 Å, particle size 40-60μm) as stationary phase. Gradients of the mobile phase are specified for each compound.

NMR spectra were recorded at room temperature (RT) with a 400 MHz Bruker NMR spectrometer for routine experiments. The chemical shifts (δ) are reported in ppm relative to the solvent signal in ^{1}H NMR. Coupling constants (J) are reported in Hertz (Hz). The following abbreviations are used to define the multiplicity in ^{1}H NMR spectra: s = singlet, d = doublet, t = triplet, m = multiplet, dd = doublet of doublets, ca= complex absorption. FIA-HRMS analysis was performed with Waters Bioaccord LC-MS system. Specific optical rotations were recorded on a digital Perkin-Elmer 34 polarimeter at 25 ºC in a 1 mL cell. A sodium light lamp was used (589 nm). Results of specific optical rotation are reported in $dg^{-1}\,cm^3\,g^{-1}$ ($[\alpha]^{20}_D$) and concentrations (c) are expressed in $g\,cm^{-3}$.

5.2. PREPARATION OF GARNER'S ALCOHOL [*TERT*-BUTYL (*R*)-4-(HYDROXYMETHYL)-2,2-DIMETHYLOXAZOLIDINE-3-CARBOXYLATE (2)]

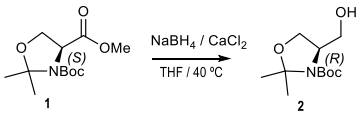

Under Ar atmosphere, 21.90 g (197 mmol) of dried $CaCl_2$ and 25.230 g (667 mmol) of $NaBH_4$ were added carefully to a solution containing 360 mL of anhydrous THF (tetrahydrofuran) and 41.06 g (159 mmol) of **1.** The mixture was stirred for 3 weeks, slightly warming.

The solution was added carefully to a 1M citric acid solution with ice (under stirring) and extracted with ethyl acetate (AcOEt), 5 x 100 mL. The organic phase was washed with 150 mL of a $NaHCO_3$ saturated solution and 150 mL of a NaCl saturated solution, dried over $MgSO_4$ and filtrated. AcOEt was evaporated under reduced pressure and the residue was purified by flash column chromatography with hexane/AcOEt, eluting with a 5% gradient increase of AcOEt up to 70%. A white to off-white solid (**2,** 26.71 g, 75% yield) was obtained.

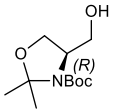

Compound **2**: White to off-white solid(mixture of rotamers). ^{1}H NMR ($CDCl_3$, 400 MHz): δ 4.14-3.91 (m, 2H), 3.85-3.67 (m, 2H), 3.59 (s, 1H), 1.53 (s, 6H), 1.42 (s, 9H). ^{13}C NMR ($CDCl_3$, 101 MHz): δ 94.1, 65.2, 59.5, 28.3, 27.7, 27.1, 24.6.

5.3. PREPARATION OF GARNER'S ALDEHYDE

5.3.1 Synthesis of IBX (o-iodoxybenzoic acid)

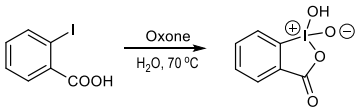

IBX was prepared from the procedure described by Frigerio & Santagostino, 1999. In a 2 L Erlenmeyer flask, 52.34 g (211 mmol) of 2-iodobenzoic acid were added to a solution of 198 g (322 mmol) of Oxone ($2KHSO_5$-$KHSO_4$-K_2SO_4) in 500 mL of deionized water. The mixture was stirred at 70 ºC during 3 h and cooled down using an ice batch at 5 ºC for 30 min. The resulting solid was filtrated using a 10µm filter, washed with water and acetone, and dried under vacuum. IBX was obtained as a dry white solid (40.39 g, 69% yield).

5.3.2 Synthesis of *tert*-butyl (*S*)-4-formyl-2,2-dimethyloxazolidine-3-carboxylate (3)

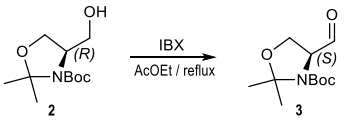

In a 500 mL round bottom flask, 13.16 g (57 mmol) of dried **2** were dissolved in 300 mL of AcOEt. The solvent was previously purged to avoid the presence of oxygen and further oxidation to the carboxylic acid. While stirring, 22.35 g (80 mmol) of dried IBX were added to the described solution and the mixture was refluxed under Ar atmosphere for 24 h.

The precipitated white insoluble solid (2-iodobenzoic acid) was removed by filtration using a 10 µm filter and washed with AcOEt. The organic solvent was evaporated under reduced pressure and the residue (oil), was purified by flash column chromatography by using hexane/AcOEt and eluting with a 3% gradient increase of AcOEt up to 30%. A clear pale yellow oil was obtained (**3**, 10.77 g, 83% yield).

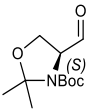

Compound **3:** Clear pale yellow oil (mixture of rotamers). ^{1}H NMR ($CDCl_3$, 400 MHz): δ 9.54 (s, 1H), 4.37-4.14 (m, 1H), 4.14-3.98 (m, 2H), 1.58 (s, 6H), 1.43 (s, 9H).

5.4. OLEFINATION

5.4.1 Synthesis of triphenyl(tetradecyl)phosphonium bromide

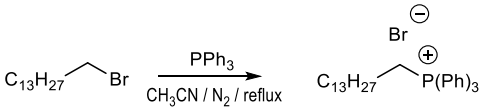

In a 500 mL round bottom flask, 25.10 g (96 mmol) of dried triphenylphosphine were dissolved in 300 mL of anhydrous CH_3CN. While stirring, 25 mL (23.3 g, 84 mmol) of 1-bromotetradecane were added to the solution under N_2 atmosphere. The mixture was refluxed in these conditions for 4 days. The resulting phosphonium salt was separated from the starting products by washing the solid with hexane and decanting the solvent (x 4 times). The remaining organic solvent was evaporated under reduced pressure and the resulting solid was dried under vacuum for 24 h. The phosphonium salt (39.61 g, 87% yield) was obtained as a colorless to pale yellow viscous liquid.

5.4.2 Wittig reaction. Synthesis of *tert*-butyl (*R,Z*)-2,2-dimethyl-4-(pentadec-1-en-1-yl)oxazolidine-3-carboxylate (4a) and *tert*-butyl (*R,E*)-2,2-dimethyl-4-(pentadec-1-en-1-yl)oxazolidine-3-carboxylate (4b)

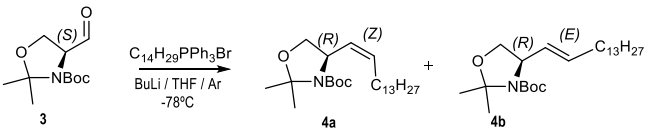

In a 500 mL round bottom flask, 36.61 g (67.85 mmol) of triphenyl(tetradecyl)phosphonium bromide were completely dissolved in 300 mL of anhydrous THF with the aid of sonication to favor the stirring. The mixture was brought to -78 ºC under Ar atmosphere and 25 mL (62.5 mmol) of a 2.5M BuLi solution in hexanes were added dropwise. The solution adopted an orange red color, was allowed to warm to 0 ºC and was stirred for 0.5 h. The reaction temperature was then lowered at -78 ºC and 11.80 g (50.5 mmol) of Garner's aldehyde (**3**), dissolved in 10 mL of THF, were added dropwise to the mixture. At that point, an attenuation of the red color was observed. The reaction was left overnight.

Next day, 200 mL of deionized water were added. The reaction crude was extracted with AcOEt (3 x 100 mL) and the organic layer was washed with water (3 x 50 mL). The organic extract was dried over anhydrous $MgSO_4$ and filtered, and the organic solvent was evaporated under reduced pressure. The residue was purified by flash column chromatography eluting with an isocratic elution (97:3 hexane/AcOEt). The relation of isomers was 9:1 for *Z* (first eluted isomer) and *E* (last eluted isomer). Isomer *Z* (**4a**, 11.572 g, 56% yield) and isomer *E* (**4b,** 1.286 g, 6% yield) were obtained as colorless syrups.

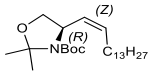

Compound **4a**: Colorless syrup. $[\alpha]_D^{25}$ +53.5º (*c* 1.0, $CHCl_3$). ^1H NMR ($CDCl_3$, 400 MHz): δ 5.48-5.31 (m, 2H), 4.71-4.47 (m, 1H), 4.04 (dd, *J* = 8.6, 6.3 Hz, 1H), 3.62 (dd, *J* = 8.6, 3.3 Hz, 1H), 2.18–1.99 (m, 2H), 1.58 (s, 3H), 1.51 (s, 3H), 1.43 (s, 9H), 1.25 (s, 22H), 0.87 (t, *J* = 6.9 Hz, 3H). ^{13}C NMR ($CDCl_3$, 101 MHz): δ 152.0, 133.8, 128.6, 93.5, 79.2, 69.1, 54.6, 32.0, 29.8, 29.4, 28.6, 27.5, 24.2, 22.8, 14.2. FIA-HRMS (ESI): *m/z* calc. for $C_{25}H_{48}NO_3$ $[M+H]^+$ 410.3629; found 410.3629.

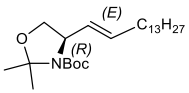

Compound **4b**: Colorless syrup. $[\alpha]_D^{25}$ +1.02º (*c* 2.0, $CHCl_3$). ^1H NMR ($CDCl_3$, 400 MHz): δ 5.66– 5.33 (m, 2H), 4.35–4.14 (m, 1H), 4.00 (dd, *J* = 8.7, 6.1 Hz, 1H), 3.70 (dd, *J* = 8.7, 2.0 Hz, 1H), 2.04 – 1.95 (m, 2H), 1.59 (s, 3H), 1.49 (s, 3H), 1.45 (s, 9H), 1.25 (s, 22H), 0.87 (t, *J* = 6.8 Hz, 3H). ^{13}C NMR ($CDCl_3$, 101 MHz): δ 151.9, 132.7, 129.0, 93.6, 79.2, 68.5, 59.2, 32.0, 29.6, 29.1, 28.4, 27.4, 23.7, 22.7,14.1. FIA-HRMS (ESI): *m/z* calc. for $C_{24}H_{48}NO_3H^+$ $[M+H]^+$ 410.3629; found 410.3630.

5.5. DIHYDROXYLATION OF OLEFINS

5.5.1 Synthesis of *tert*-butyl (*S*)-4-((*1S,2R*)-1,2-dihydroxypentadecyl)-2,2-dimethyloxazolidine-3-carboxylate (5a) and *tert*-butyl (*S*)-4-((*1R,2S*)-1,2-dihydroxypentadecyl)-2,2-dimethyloxazolidine-3-carboxylate (5b)

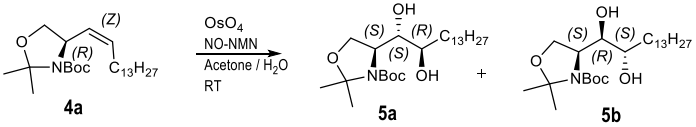

In a 500 mL round bottom flask, 8.40 g (20.47 mmol) of dried (*R,Z*)-2,2-dimethyl-4-(pentadec-1-en-1-yl)oxazolidine-3-carboxylate (**4a**) were added to 200 mL of an 8:1 acetone/water solution. In 20 mL of warm *tert*-butanol, 57 mg (0.224 mmol) of OsO_4 were dissolved and added to the mixture together with 10 mL of NMO (*N*-methylmorpholine *N*-oxide) 50% aqueous solution (48.22 mmol). The reaction crude was stirred for 24 h at room temperature.

To the reaction mixture, 7.5 g (59.50 mmol) of Na_2SO_3 were added and it was stirred for 30 min. The crude was extracted with AcOEt, dried over $MgSO_4$ and filtered. The organic extract was evaporated under reduced pressure and the residue was purified by column chromatography eluting with hexane/AcOEt with a 1% gradient increase of AcOEt up to 30%. The first eluted diastereomer, (**5b,** 1.297g, 14% yield) was obtained as a colorless syrup and last eluted diastereomer (**5a,** 5.657 g, 61% yield) was obtained as a white wax.

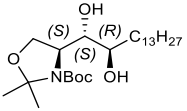

Compound **5a**: White wax. $[\alpha]_D^{25}$ - 5.11 (*c* 1.0, $CHCl_3$). ^1H NMR ($CDCl_3$, 400 MHz): δ 4.22–4.08 (m, 2H), 3.96-3.77 (ca, 1H), 3.67–3.51 (m, 2H), 3.40 (dd, *J* = 3.0, 6.8 Hz, 1H), 1.63 (s, 1H), 1.57 (s, 3H), 1.49 (s, 3H), 1.47 (s, 9H), 1.39–1.16 (m, 22H), 0.86 (t, *J* = 6.8 Hz, 3H). ^{13}C NMR ($CDCl_3$, 101 MHz): δ 93.8, 81.1, 74.6, 73.9, 65.0, 59.1, 33.2, 31.8, 29.6, 28.3, 26.7, 26.2, 24.0, 22.6, 14.0. FIA-HRMS (ESI): *m/z* calc. for $C_{25}H_{50}NO_5^+$ $[M+H]^+$ 444.3684; found 444.3689.

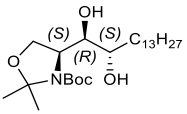

Compound **5b**: Colorless syrup. $[\alpha]_D^{25}$ -21.1 (*c* 1.0, $CHCl_3$). ^1H NMR ($CDCl_3$, 400 MHz): δ 4.40 – 4.27 (m, 2H), 4.12-4.07 (ca, 1H), 3.98-3.76 (ca, 1H), 3.49 – 3.20 (m, 2H), 1.70 (s, 2H), 1.61 (s, 3H), 1.52 (s, 3H), 1.50 (s, 9H), 1.25 (s, 21H), 0.87 (t, J = 6.3 Hz, 3H).^{13}C NMR ($CDCl_3$, 101 MHz): δ 154.82, 94.4, 81.5, 78.4, 71.5, 66.7, 57.4, 32.6, 29.6, 29.2, 28.1, 26.3, 25.6, 23.9, 22.6, 14.0. FIA-HRMS (ESI): *m/z* calc. for $C_{25}H_{50}NO_5^+$ $[M+H]^+$ 444.3684; found 444.3680.

5.6. PHYTOSPHINGOSINE DEPROTECTION

5.6.1 Synthesis of (*2S,3S,4R*)-2-aminoheptadecane-1,3,4-triol (6)

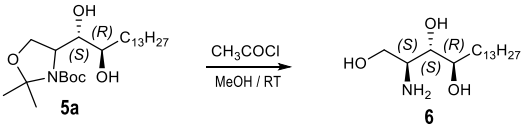

In a 250 mL round bottom flask, 1.013 g (2.283 mmol) of dried **5a**, 1 mL (14 mmol) of CH_3COCl and 75 mL of methanol (MeOH) were introduced. The mixture was left to stir for 24 h at room temperature.

The organic solvent was evaporated under reduced pressure. The obtained residue was concentrated under reduced pressure with 20 mL of MeOH (x3 times), evaporating each time the solvent to remove secondary products such as methyl acetate (CH_3COOMe) and acetone. A basic treatment was performed adding 1 mL of 30% NH_3 in 20 mL of MeOH over the residue and removing each time the organic extract. The treated residue was purified by column chromatography eluting with a warm dichloromethane (DCM) / 3% NH_3 in MeOH solution (to solubilize and maintain the phytosphingosine in its neutral form) with a 1% increase gradient of the basified MeOH solution up to 30 %. A white wax was obtained (**6**, 520 mg, 75% yield).

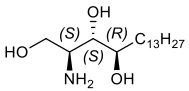

Compound **6**: White wax. ^{1}H NMR (CD_3OD, 400 MHz): δ 3.88 (dd, J = 11.2, 3.9 Hz, 1H), 3.74 – 3.66 (m, 1H), 3.55 – 3.46 (m, 2H), 3.32 – 3.25 (m, 1H), 1.84 – 1.53 (m, 2H), 1.34 (s, 22H), 0.93 (t, J = 6.8 Hz, 3H).^{13}C NMR (MeOD, 101 MHz): δ 73.5, 72.5, 59.9, 54.7, 33.8, 3.73, 29.5, 29.2, 25.1, 22.4, 13.2. FIA-HRMS (ESI): *m/z* calc. for $C_{17}H_{38}NO_3^+$ $[M+H]^+$ 304.2846; found 304.2845.

5.7. PHYTOSPHINGOSINE ACYLATION

5.7.1 Synthesis of *N*-((*2S,3S,4R*)-1,3,4-trihydroxyheptadecan-2-yl)palmitamide (7)

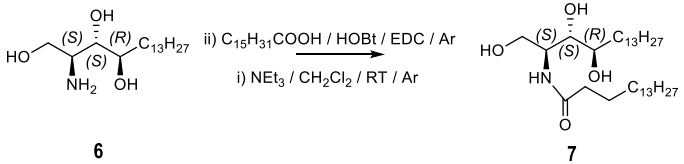

In a 50 mL round bottom flask, 520 mg (1.713 mmol) of dried **6** were dissolved in 30 mL of DCM under Ar atmosphere and stirring. Then, 700 µL (5 mmol) of TEA were added to the mixture.

A solution containing 480 mg (1.870 mmol) of palmitic acid, 256 mg (1.880 mmol) of hydroxybenzotriazole (HOBt), 433 mg (2.260 mmol) of *N*-(3-dimethylaminopropyl)-*N'*-ethylcarbodiimide (EDC) and 30 mL of DCM was prepared under Ar atmosphere. EDC was introduced after complete dissolution of HOBt and palmitic acid to avoid its reaction with the activated acid. The preparation was added dropwise to the reaction mixture (to solubilize compounds progressively). A white precipitate was observed over time as the reaction evolved. The mixture was maintained under stirring overnight and at RT.

Then, 25 mL of water were added to the reaction mixture and the reaction crude was extracted with 25 mL of $CHCl_3$ x 6, heating the organic phase until complete dissolution of the precipitate. The organic extract was evaporated under reduced pressure and the residue was purified by flash column chromatography. A pre-elution treatment performed with a 7:3 hexane/methyl *tert*-butyl ether (MTBE) solution (4 column volumes) was done to remove the excess of non-reacted palmitic acid. Final elution was carried out with DCM/MeOH 0.2 % stepwise gradient of MeOH up to 10%.

Given the excess of palmitic acid, secondary reactions forming monoester amides take place. The separated fractions of these compounds can be reversed by reaction with K_2CO_3 to obtain **7**. A white wax (**7,** 700 mg, 75% yield) was obtained.

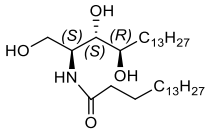

Compund **7**: White wax. ^{1}H NMR ($CDCl_3$, 400 MHz): δ 6.32 (dd, J = 7.6 Hz, 1H), 4.16–4.10 (m, 1H), 3.92 (d, J = 6.7 Hz, 1H), 3.77–3.70 (m, 1H), 3.59 (d, J = 19.9 Hz, 2H), 2.27 – 2.16 (m, 2H), 1.83-1.65 (m,2H), 1.51-1.38 (m,2H), 1.25 (s, 44H), 0.88 (t, J = 6.8 Hz, 6H). FIA-HRMS (ESI): *m/z* calc. for $C_{33}H_{68}NO_4^+$ $[M+H]^+$ 542.5143; found 542.5142.

6. RESULTS AND DISCUSSION

The synthetic route for the preparation of the described compounds is depicted (Fig. 5). It constitutes a linear synthesis that defines an absolute configuration using a derivative of L-serine as a raw material (2*S*). It implies two critical steps from the stereochemical point of view (Wittig reaction and Upjohn dihydroxylation) and the creation of two new chiral centers.

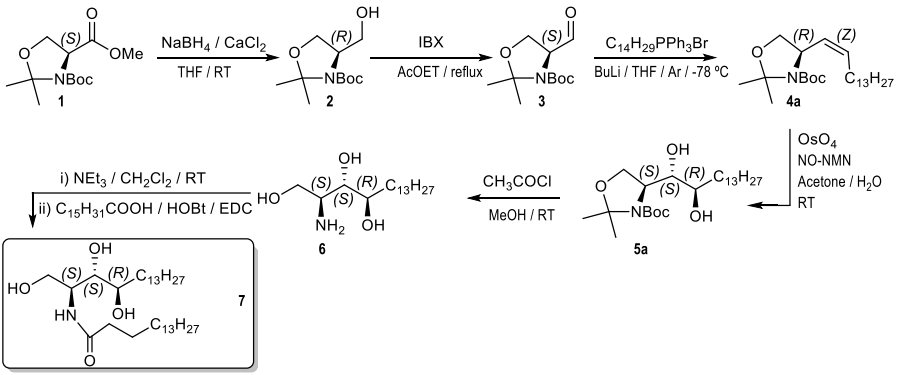

Figure 5. Synthetic route for the preparation of C17 D-*ribo*-phytosphingosine and phytoceramide.

6.1. GARNER'S ALCOHOL FORMATION: ESTER REDUCTION WITH $NaBH_4$ USING A METALLIC CATALYST

Esters are usually reduced with $LiAlH_4$, as the carbonyl is not an efficient electrophilic center and needs a powerful hydride-transfer reagent. Despite this, the starting material (**1**) contains a carbamate as a labile functional group that would react if $LiAlH_4$ were to be used as a reduction agent. That is the reason why a more selective and milder reagent needs to be utilized(Hager, 2020).

In this case, sodium borohydride ($NaBH_4$) is used together with $CaCl_2$. The first one corresponds to the reductant, which is not capable of deprotecting the amine, and the second one provides the metallic catalyst, calcium cation (Ca^{2+}) (Yurkanis Bruice, 2008, p. 1072). This is

attributed to the availability of the counterion for coordination to the substrate, thus making the carbonyl more electrophilic and promoting reduction(Hager, 2020). In addition, anhydrous $CaCl_2$ can act as desiccating agent and favor the absence of water.

Another important point in this reaction is the proper concentration of $NaBH_4$ in the organic aprotic solvent (in this case THF) given that a saturated solution affords a very low presence of the reactive in the reaction media.

There is evidence (Passiniemi & Koskinen, 2013) for the obtention of Garner's aldehyde starting from **1** through the use of DIBALH without prior reduction, although the yield for this reaction is considerably low.

6.2. IBX OXIDATION

IBX is a mild oxidant for the conversion of alcohols to aldehydes or ketones. It is virtually insoluble in most organic solvents; indeed, this solid-phase reagent simplifies the separation of oxidation byproducts and facilitates recovery and reuse of the oxidant. AcOEt is the solvent of choice because it is inert, and all byproducts are insoluble in it at room temperature, such that a highly pure compound is obtained beyond a simple filtration(More & Finney, 2002).

On the other hand, this oxidation in primary alcohols (as well as stronger oxidations with cromic o dicromic acids) initially generates an aldehyde. Nevertheless, the reaction does not stop there. Instead, the aldehyde undergoes further oxidation to the respective carboxylic acid (also by the presence of air and O_2). As an alternative, an additional oxidation method involving PCC (pyridinium chlorochromate) as oxidizing agent using DCM as solvent exists(Corey & Suggs, 1975).

However, due to the toxicity of chromium-based reagents, other methods have been developed to oxidize alcohols. One of the most used is the so-called Swern oxidation, involving dimethyl sulfoxide [$(CH_3)_2SO$], oxalyl chloride [$(COCl)_2$] and triethylamine (TEA). Since the reaction does not take place in aqueous solution, the oxidation of a primary alcohol is stopped at the aldehyde (as in the reaction with PCC) (Yurkanis Bruice, 2008, Chapter 19).

Even so, the use of dimethyl sulfoxide is environmentally controversial and in addition 2-iodobenzoic acid (the precipitated side product) can be recycled to re-obtain IBX.

In conclusion, the use of IBX is preferable for the oxidation of alcohols, as it is a gentle, environmentally friendly process (it is also possible to recover the starting reagent) and provides

a practically pure product due to the ease of separation from the reaction medium. Conversely, it is advisable to work in approximately stoichiometric quantities and to reduce the reaction time to avoid oxidation of the aldehyde to the carboxylic acid (as this would require purification).

The action mechanism of IBX in primary alcohols oxidation is described (Fig. 6). It consists of an initial deprotonation of the alcohol and a subsequent nucleophilic attack by the alcohol on the iodine atom, which acts as an electrophile, with a consequent release of a water molecule. The formed intermediate deprotonates the adjacent carbon to the alcohol group in an intramolecular reaction, generating the aldehyde(Kaur & Ariafard, 2020).

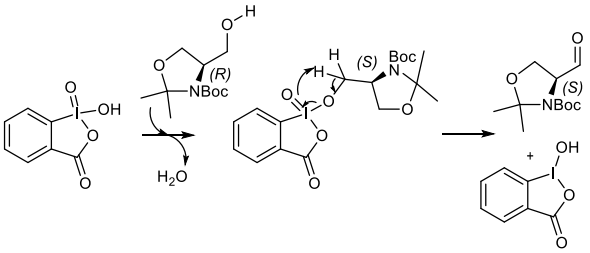

Figure 6. IBX oxidation mechanism in primary alcohols.

6.3. OLEFINATION: WITTIG REACTION

6.3.1 Phosphonium salt formation

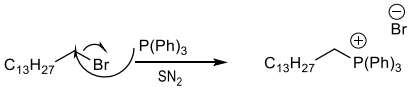

Figure 7. S_N2 reaction mechanism for phosphonium salt formation.

The reaction consists of a bimolecular nucleophilic substitution (S_N2) of the triphenylphosphine by the bromide at the terminal electrophile carbon since the halide attracts high electron density to itself. A polar aprotic solvent is used, in this case CH_3CN, which is capable of surrounding the nucleophile while allows it to attack the substrate(Yurkanis Bruice, 2008, pp. 346–352).

6.3.2 Wittig reaction mechanism

This is the preparation of an alkene from an aldehyde and an ylide generated from a phosphonium salt using a strong base, in this case BuLi (n-butyllithium). The resulting ylide is stabilized by resonance, as a resonance form involving the formation of a double bound can be written.

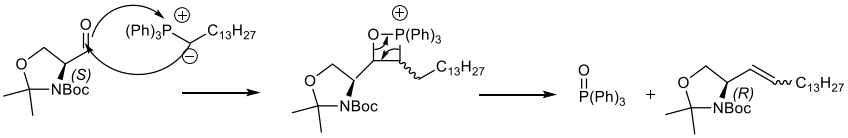

Figure 8. General mechanism of the desired Wittig reaction.

The first step of the mechanism is a [2+2] cycloaddition (a pericyclic reaction), forming an oxaphosphetane intermediate while the second is a cycloreversion. The driving force is the formation of phosphorous oxide, a very stable compound(Li, 2021).

If the ylide contains an electron attracting group it will be stabilized and the reaction will preferentially give the *E* isomer, whereas a non-stabilized ylide, which does not contain an attracting group, will mostly give the *Z* isomer(Li, 2021).

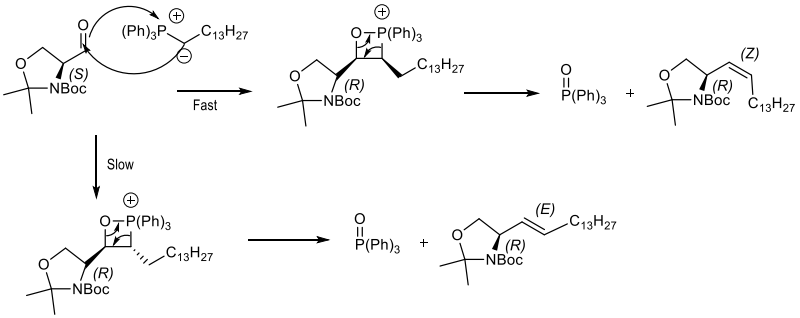

Figure 9. Specified mechanism of [2+2] cycloaddition for stabilized and non-stabilized ylides.

In this case, the starting point was a non-stabilized ylide, and therefore the *Z*-isomer was expected to be obtained. This fact was favored by performing the reaction at -78 ºC to help the kinetic product form, predominantly. This would subsequently allow the synthesis of the phytosphingosine with the desired absolute configuration.

As a result of the reaction, both isomers, *Z* and *E*, were separated and individually obtained. In order to identify them, two criteria were used: stereoselectivity ratio and chromatographic behavior. It was considered that the *Z* isomer would correspond to the predominant compound,

given the characteristics of the formed ylide. The isomers were obtained with a 9:1 ratio. The specific optical rotation was then determined for each compound and compared with the results found in the literature for the *Z* and *E* isomers of a C18 olefin(Azuma et al., 2000):

Isomer	Specific optical rotation (º)	Assigned Isomer	Specific optical rotation for corresponding olefin C18 isomer (º)
Major (9)	+53.5	*Z*	+55.9
Minor (1)	+1.02	*E*	-4.63

Table 1. Comparison and identification of isomers on the basis of their specific optical rotation.

In both cases, a similar tendency was observed for the specific optical rotation. The results were comparable for the *Z*-isomer but slightly different for the *E*-isomer. It should be noted that, in the chromatographic separation, the first eluted compound was the major one, with the consequent fact that the minor product might contain a certain amount of the first one. This influences the measurement, since the major isomer has a specific optical rotation of a considerable absolute value, and positive, as compared to the minor compound, whose value is low and negative. Thus, considering that the *E*-isomer contained at least a 5% of the *Z*-isomer, the obtained result would be equally positive.

On the other hand, ^{1}H NMR analysis gave similar results for both compounds. Since the signals for the hydrogens on the carbons forming the double bonds overlap, it has not been possible to determine the corresponding coupling constants. Analysis of the ^{13}C NMR spectrum showed that chemical displacements of the alpha-positioned carbons with respect to the double bond are remarkably different for both stereoisomers. ChemDraw chemical shifts prediction for ^{13}C NMR matched the obtained experimental absorptions for each configuration.

In addition, the signals corresponding to the *Z* isomer can be observed in the baseline of the spectrum of the *E* isomer with very low intensity, which proves the presence of a small amount of the first in the latter. This is consistent with the results of the specific optical rotation, as already explained, which does not represent a problem since the isomer of interest is the compound with

Z stereochemistry. Hence, the result of the measurement agrees with the experimental facts and relates to the bibliographical data.

However, it should be noted that some carbon signals are splitted, due to the presence of the *tert*-butoxycarbonyl group, which is explained by the existence of preferred conformations at RT.

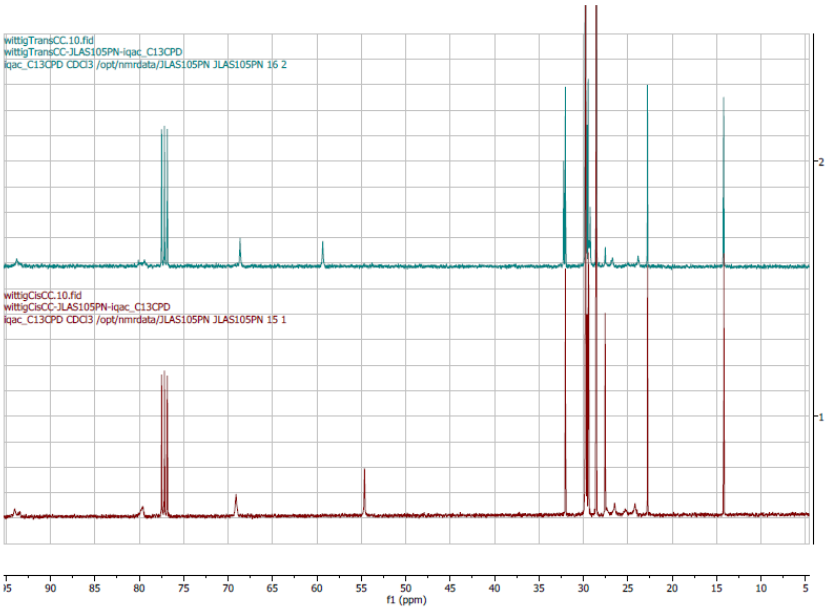

Figure 10. Superposed spectra of the *E*-isomer (upper diagram) and the *Z*-isomer (lower diagram).

6.4. DIHYDROXYLATION OF OLEFINS

6.4.1 Upjohn dihydroxylation

The Upjohn dihydroxylation is a *syn*-selective preparation of 1,2-diols from alkenes using osmium tetroxide (OsO_4) and a stoichiometric amount of an oxidant, *N*-methyl morpholine *N*-Oxide (NMO). A [3+2] pericyclic cycloaddition takes place:

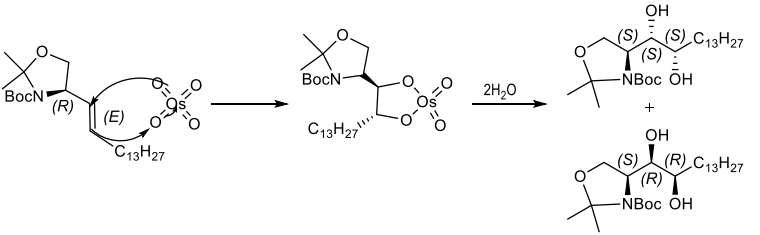

Figure 11. [3+2] Cycloaddition mechanism for the Upjohn dihydroxylation with the *E*-isomer.

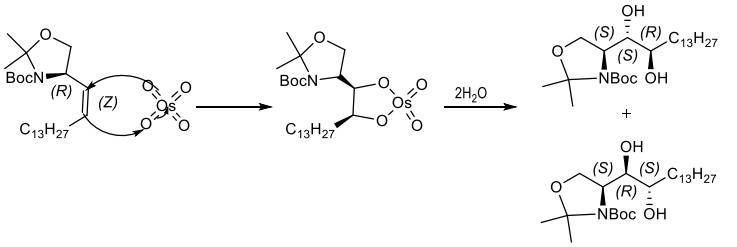

Figure 12. [3+2] Cycloaddition mechanism for the Upjohn dihydroxylation with the *Z*-isomer.

OsO_4 is a toxic, volatile, and polluting compound. To prevent an excessive use, it reacts in catalytic quantities and is treated with NMO. This oxide regenerates OsO_4 according to the catalytic cycle (Fig. 13).

Initially, the oxidation state of Os corresponds to VIII. Immediately after cycloaddition, it is reduced to VI. At this point, NMO can oxidise the metal back to the original state, generating *N*-methylmorpholine in turn. For this reason, it is important to always have NMO at least in stoichiometric quantities.

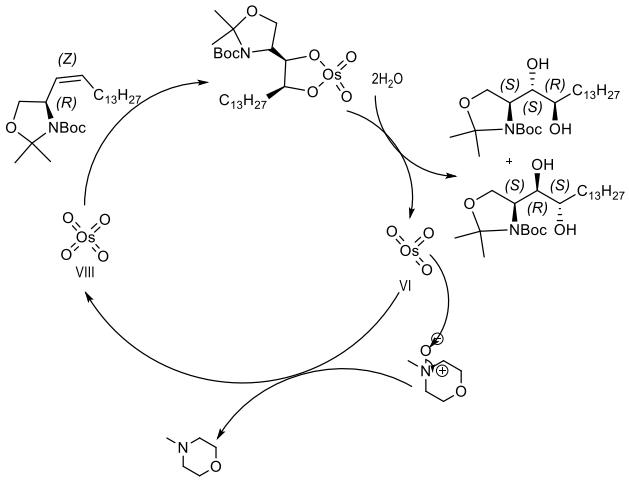

Figure 13. Catalytic cycle for OsO_4 regeneration.

As illustrated (Fig. 11 and 12), different products are obtained depending on the configuration of the employed alkene, considering that the precursor is enantiomerically pure.

Separation of the olefin stereoisomers made possible to study the individual dihydroxylation for each of them. Thus, two different diastereomers were obtained in each case (as could be observed by monitoring both reactions with TLC) due to *syn*-addition of OsO_4 and the existence of a chiral center in the amine position with absolute 2*S* configuration (Fig. 14).

Protected phytosphingosine diastereomers (absolute configuration)	**Dihydroxylation of 4a**	**Dihydroxylation of 4b**
2S,3S,4R	Y	N
2S,3R,4S	Y	N
2S,3S.3S	N	Y
2S,3R,3R	N	Y

Table 2. Description of the obtained dihydroxylation products for each compound.

With these results, dihydroxylated compounds from *Z*-olefin **4a** were separated by flash column chromatography and characterized by specific optical rotation, MS and ^{1}H and ^{13}C NMR analysis. For the compounds obtained by reaction of *E*-olefin **4b**, characterization was not carried out since they were not the objectives of this work. The separation of these 4 compounds, however, means that all the different phytosphingosine diastereomic forms are possible to isolate and therefore available for the synthesis of different sphingolipid intermediates and jaspines.

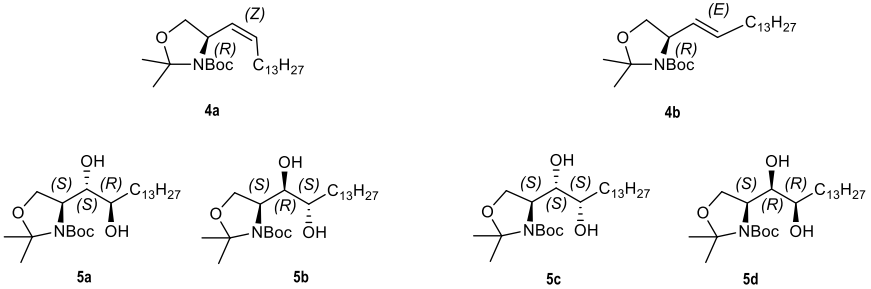

*Figure 14. Dihydroxylation products obtained from compunds **4a** and **4b.***

In the case of the dihydroxylation of the *Z*-isomer, the literature (Azuma et al., 2000) describes the obtention of the desired configurational diastereomer in a 4:1 ratio to respectively give rise to protected C18 D-*ribo*-phytosphingosine and D-*arabino*-phytosphingosine. The solvent that provides these results is a 8:1 acetone/water mixture together with the dissolution of OsO_4 in *tert*-butanol, which is necessary to obtain the desired diastereomeric ratio.

Experimentally, two diastereomers were also obtained in the same conditions. In the chromatographic separation, the minor compound was eluted first whereas the major was the second one. With the aim of identifying the obtained compounds, their ratio (determined from the amounts obtained of each compound after purification) and NMR spectra (^{1}H and ^{13}C) were evaluated, and the specific optical rotation was measured. These results were compared with those described in the literature for the corresponding C18 diastereomers (Azuma et al., 2000), observing a similar tendency in their specific optical rotation.

Diastereomer	Specific optical rotation (º)	Assigned compound	Specific optical rotation for corresponding C18 diastereomer (º)
Major (4)	-5.11	5a	-5.36
Minor (1)	-21.1	5b	-30.3

Table 3. Comparison and identification of diastereomers on the basis of their specific optical rotation.

The results are consistent for the case of the major compound, which can be associated to protected C17 phytosphingosine with D-*ribo*-stereochemistry (**5a**). For the minor diastereomer, a slight variation from the reference value exists but it can be anyway assigned to C17 phytosphingosine with D-*arabino*-stereochemistry (**5b**) due to the consistency of NMR shifts with the ones found in the literature. Additionally, the exact mass of the compounds was determined by MS.

6.5. PHYTOSPHINGOSINE DEPROTECTION

Traditional approaches for *N*-^{t}Boc deprotection rely on trifluoroacetic acid (TFA) cleavage. Other strategies include the use of metal catalysts, removal with HCl in organic solvents or with acetyl chloride in MeOH, which generates HCl through an acyl nucleophilic substitution (Fig 15), (George et al., 2020).

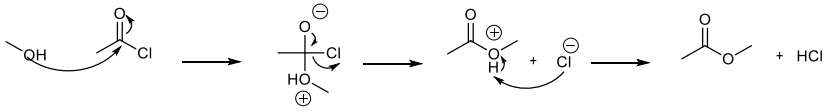

Figure 15: Acyl nucleophilic substitution of CH_3COCl with MeOH to form CH_3COOMe and HCl.

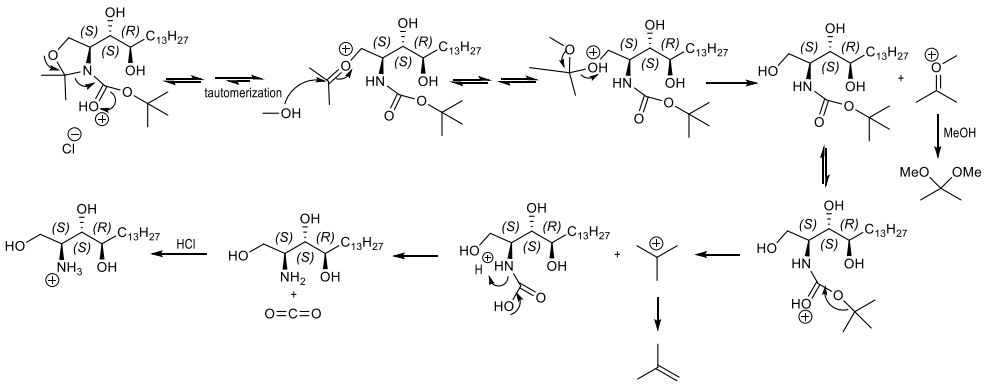

Figure 16: Mechanism of *N*-^{t}Boc and isopropylidene removal.

HCl quantitatively generated *in situ* by the addition of acetyl chloride to alcoholic solutions is a useful reagent for N-^{t}Boc group deprotection(Nudelman et al., 1998). In this case, we used acyl chloride (CH_3COCl) and MeOH at RT to perform this reaction. Acetone dimethylacetal is first formed as a result of the removal of the isopropylidene protecting group. In a second stage N-^{t}Boc group removal, with the formation of gaseous products (isobutylene and carbon dioxide) which evolve and shift the equilibrium to product formation. It is important to perform a basic treatment in order to release the protonated amine, in addition to eliminating the CH_3COOMe formed (a liquid with a low boiling point) under reduced pressure. The mechanism is the same as for the elimination reaction with TFA but the chosen method is a milder alternative to the use of a strong acid.

In this reaction, it has been important to ensure that all the starting material was completely deprotected, since an intermediate product in which only the isopropylidene group is removed can be isolated.

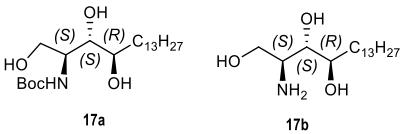

Figure 17: **17a** corresponds to partially deprotected product and **17b** to total deprotection.

6.6. PHYTOSPHINGOSINE ACYLATION

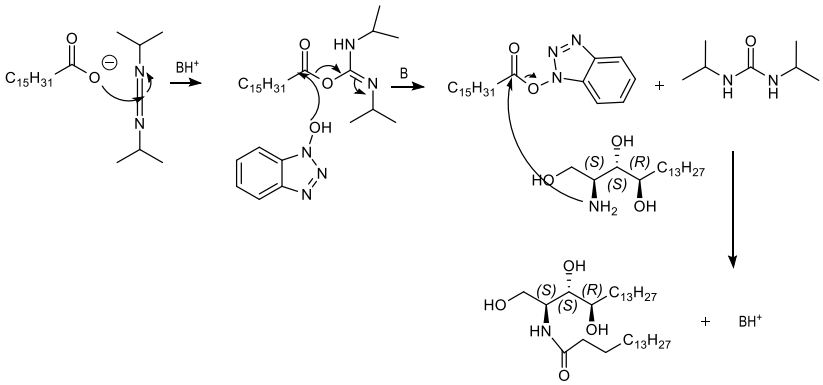

Figure 18. Mechanisme of phytosphigosine acylation.

The final step involves the acylation of phytosphingosine. This is carried out using an activating agent (EDC, *N*-(3-dimethylaminopropyl)-*N*-ethylcarbodiimide hydrochloride), which

forms a more electrophilic carbonyl group that reacts with hydroxybenzotriazole (HOBt), a nucleophilic catalyst the use of which avoids racemization. This facilitates the attack by the phytosphingosine amino group to form the target amide, forming 1,3-diisopropylurea as a secondary product. TEA is used as base(Schrader et al., 2009).

Acylation entails further formation of amide monoesters, as the alcohols are not protected. This problem was encountered in this reaction; therefore, a chromatographic purification was needed. The fractions corresponding to these compounds were submitted to saponification using K_2CO_3 in methanol to increase the amount of final product.

An alternative that could avoid this problem would be a transient protection method of the free alcohols as trimethylsilyl ethers (TMS). Thus, a treatment with chlorotrimethylsilane in presence of a tertiary amine gives rise to the corresponding silyl ethers. This reaction is favoured with the use of palmitic acid activated as its acid chloride, $CH_3(CH_2)_{14}COCl$, to promote a more reactive acyl nucleophilic substitution. The amine prevents the solution from becoming acidic by reacting with the HCl generated in the reaction. TMS ether, which is stable in neutral and basic solutions, can be removed with aqueous acid under mild conditions (Yurkanis Bruice, 2008, p. 820).

Although a tertiary Si atom is used, a S_N2 reaction is possible. While a tertiary alkyl halide does not take part in S_N2 reactions, the tertiary silyl compound does (since Si-C bonds are longer than C-C bonds and steric hindrance at the site of nucleophilic attack is reduced)(Yurkanis Bruice, 2008, p. 820).

The final C17 phytoceramide with D-*ribo*-stereochemistry (**7**) was obtained in a quantity of 700 mg and characterized through ^{1}H NMR. The characteristics of the final product generated several drawbacks, as the compound is not easily soluble in common solvents (it has a wax consistency). This made it difficult to obtain a ^{13}C NMR spectrum, considering that a higher concentrated sample is needed, which is why the product was only characterized by ^{1}H NMR analysis and its exact mass determined by FIA-HRMS.

A C18 phytoceramide probe was prepared in similar conditions from the respective commercially available phytoceramide and was compared to the final product by ^{1}H NMR analysis:

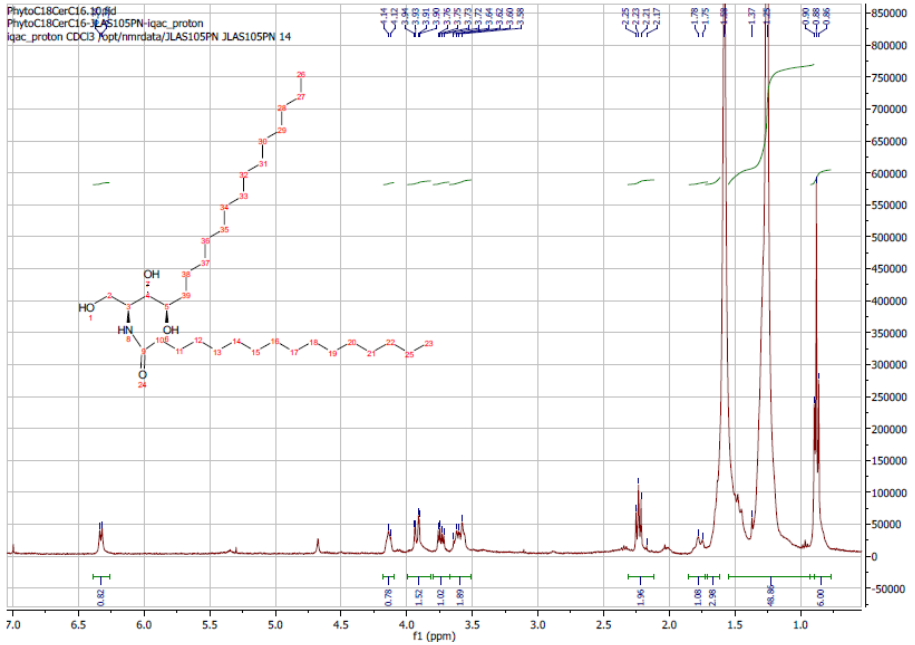

Figure 19. ^{1}H RMN spectra of C18 phytoceramide

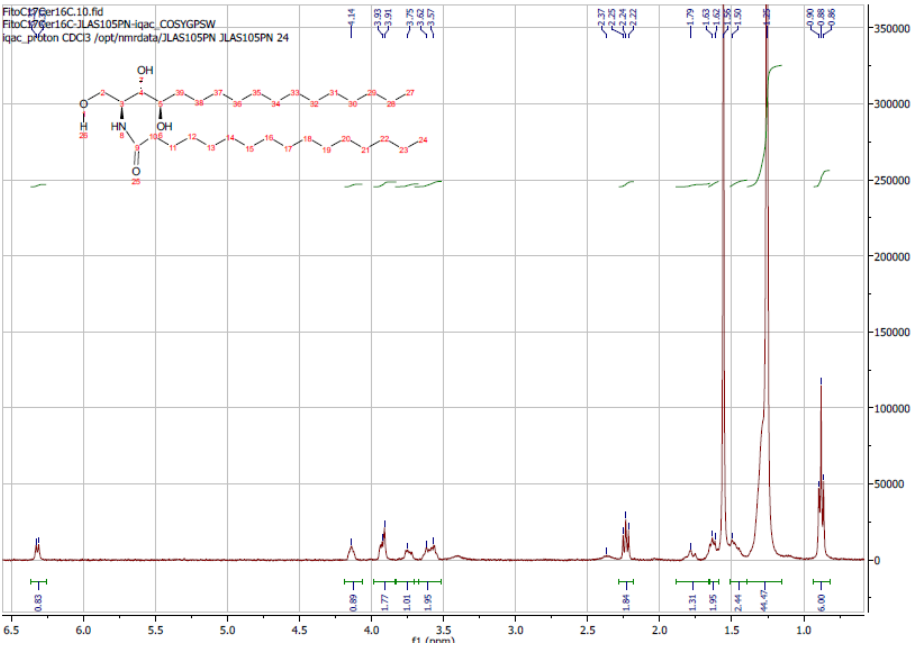

Figure 20. ^{1}H RMN spectrum of C17 phytoceramide

One can observe that the spectra (Fig. 19, Fig. 20) show a practically identical profile, with a peak of higher intensity corresponding to the alkylic protons in the case of phytoceramide C18 (Fig. 19), as it has 2 more hydrogens. This leads to the ultimate characterization of the obtained product.

7. CONCLUSIONS

The methodology implies an exhaustive control in the following critical stages, in order to simplify synthesis and characterization:

- Chromatographic separation of *Z* and *E* isomers in the Wittig reaction
- Stereoselectivity control in the Upjohn dihydroxylation
- Chromatographic separation of diastereomers

As discussed, stereo and diastereoselectivity in these reactions are not high enough to obtain a single species without chromatographic purification. It must be noted that a mixture of compounds can provide ambiguous results, leading to costly characterizations. A strict chromatographic separation is required, which provides an easy differentiation of the obtained products by only measuring their optical rotation.

An advantage for the characterization of the final product is that its ^{1}H NMR spectrum can be compared with that of a reference spectrum, in this case phytoceramide C18, for easier identification.

Regarding the principal objective of the study, to obtain the required quantities of the compounds, has been achieved. On the other hand, the downside to be taken into account is the costly and difficult handling of the final product, which is hardly soluble in MeOH and $CHCl_3$. This point may be considered and solved by performing the acylation proces*s in situ* when administering the truncated probes to mice.

In short and leaving aside the more costly aspects of the process, it is a reproducible synthetic methodology. For this reason, it is considered feasible to supply the compound by means of this procedure, being less expensive than purchasing it. In addition, the establishment of this synthetic route has served to introduce an entry route to the synthesis of different stereoisomers of truncated jaspine and other modified sphingolipid intermediates(Abraham et al., 2008).

8. REFERENCES AND NOTES

Abraham, E., Davies, S. G., Roberts, P. M., Russell, A. J., & Thomson, J. E. (2008). Jaspine B (pachastrissamine) and 2-epi-jaspine B: synthesis and structural assignment. *Tetrahedron Asymmetry*, *19*(9), 1027–1047.

Azuma, H., Tamagaki, S., & Ogino, K. (2000). Stereospecific total syntheses of sphingosine and its analogues from L- serine. *Journal of Organic Chemistry*, *65*(11), 3538–3541.

Barbarroja, N., Rodriguez-Cuenca, S., Nygren, H., Camargo, A., Pirraco, A., Relat, J., Cuadrado, I., Pellegrinelli, V., Medina-Gomez, G., Lopez-Pedrera, C., Tinahones, F. J., Symons, J. D., Summers, S. A., Oresic, M., & Vidal-Puig, A. (2015). Increased dihydroceramide/ceramide ratio mediated by defective expression of degs1 impairs adipocyte differentiation and function. *Diabetes*, *64*(4), 1180–1192.

Boini, K. M., Zhang, C., Xia, M., Poklis, J. L., & Li, P. L. (2010). Role of sphingolipid mediator ceramide in obesity and renal injury in mice fed a high-fat diet. *Journal of Pharmacology and Experimental Therapeutics*, *334*(3), 839–846.

Canals, D., Mormeneo, D., Fabriàs, G., Llebaria, A., Casas, J., & Delgado, A. (2009). Synthesis and biological properties of Pachastrissamine (jaspine B) and diastereoisomeric jaspines. *Bioorganic and Medicinal Chemistry*, *17*(1), 235–241.

Corey, E. J., & Suggs, J. W. (1975). Pyridinium chlorochromate. An efficient reagent for oxidation of primary and secondary alcohols to carbonyl compounds. *Tetrahedron Letters*, *16*(31), 2647–2650.

Frigerio, M., & Santagostino, M. (1999). A User-Friendly Entry to 2-Iodoxybenzoic Acid (IBX). *J. Org. Chem*, *64*, 4537–4538.

George, N., Ofori, S., Parkin, S., & Awuah, S. G. (2020). Mild deprotection of the: N-tert - butyloxycarbonyl (N -Boc) group using oxalyl chloride. *RSC Advances*, *10*(40), 24017–24026.

Hager, W. H. (2020). Chemistry 115 Handouts. In *Reduction* (pp. 638–639). Harvard University.

Howell, A., & Ndakala, A. (2005). The Preparation and Biological Significance of Phytosphingosines. *Current Organic Chemistry*, *6*(4), 365–391.

Imashiro, R., Sakurai, O., Yamashita, T., & Horikawa, H. (1998). A short and efficient synthesis of phytosphingosines using asymmetric dihydroxylation. *Tetrahedron*, *54*(36), 10657–10670.

Kaur, A., & Ariafard, A. (2020). Mechanistic investigation into phenol oxidation by IBX elucidated by DFT calculations. *Organic and Biomolecular Chemistry*, *18*(6), 1117–1129.

Li, J. J. (2021). Wittig Reaction. In *Name Reactions* (pp. 570–579). Springer, Cham.

Longato, L., Tong, M., Wands, J. R., & de la Monte, S. M. (2012). High fat diet induced hepatic steatosis and insulin resistance: Role of dysregulated ceramide metabolism. *Hepatology Research*, *42*(4), 412–427.

More, J. D., & Finney, N. S. (2002). A simple and advantageous protocol for the oxidation of alcohols with o-iodoxybenzoic acid (IBX). *Organic Letters*, *4*(17), 3001–3003.

Nudelman, A., Bechor, Y., Falb, E., Fischer, B., Wexler, B. A., & Nudelman, A. (1998). Acetyl chloride-methanol as a convenient reagent for: A) quantitative formation of amine hydrochlorides; B) carboxylate ester formation; C) mild removal of N-t-Boc-protective group. *Synthetic Communications*, *28*(3), 471–474.

Pagadala, M., Kasumov, T., McCullough, A. J., Zein, N. N., & Kirwan, J. P. (2012). Role of ceramides in nonalcoholic fatty liver disease. *Trends in Endocrinology and Metabolism*, *23*(8), 365–371.

Passiniemi, M., & Koskinen, A. M. P. (2013). Garner's aldehyde as a versatile intermediate in the synthesis of enantiopure natural products. *Beilstein Journal of Organic Chemistry*, *9*(1), 2641–2659.

Régnier, M., Polizzi, A., Guillou, H., & Loiseau, N. (2019). Sphingolipid metabolism in non-alcoholic fatty liver diseases. *Biochimie*, *159*, 9–22.

Schrader, E. K., Harstad, K. G., & Matouschek, A. (2009). Targeting proteins for degradation. *Nature Chemical Biology*, *5*(11), 815–822.

Yurkanis Bruice, P. (2008). *Quimica Organica* (5th ed.). Pearson Education.

9. ACRONYMS

AcOEt: ethyl acetate

Boc: ^{t}Butoxycarbonyl

BuLi: n-butyllithium

CDase: ceramidase

CH_3COOMe: methyl acetate

CerS: ceramide synthase

CerS2: ceramide synthase 2

DCM: dichloromethane

DES1: Δ-4-dihydroceramide desaturase 1

DES2: Δ-4-dihydroceramide desaturase 2

EDC: *N*-(3-dimethylaminopropyl)-*N*'-ethylcarbodiimide

ER: Endoplasmic reticulum

FIA-HRMS: flow injection analysis coupled to resolution mass spectrometry

HRMS-HPLC: high pressurized liquid chromatography coupled to high resolution mass spectrometry

Hz: Hertz

IBX: o-iodoxybenzoic acid

J: coupling constant in NMR

KSPR: keto-sphinganine reductase

HOBt: hydroxybenzotriazole

LC-MS: líquid chromatography coupled to mass spectrometry

MeOH: methanol

MTBE: methyl *tert*-butyl ether

NAFLD: non-alcoholic fatty liver disease

NASH: non-alcoholic steatohepatitis

NMO: *N*-methylmorpholine N-oxide

RT: room temperature

S1K: sphinganine kinase

S1P: sphingosine-1-phosphate

SL: sphingolipid

SMase: sphingomyelinase

S_N2: bimolecular nucleophilic substitution

SphK: sphinganine kinase

SPT: serine palmitoyl transferase

TFA: trifluoroacetic acid

TEA: triethylamine

THF: tetrahydrofuran

TMS: trimethylsilyl ester

APPENDICES

APPENDIX: NMR SPECTRA

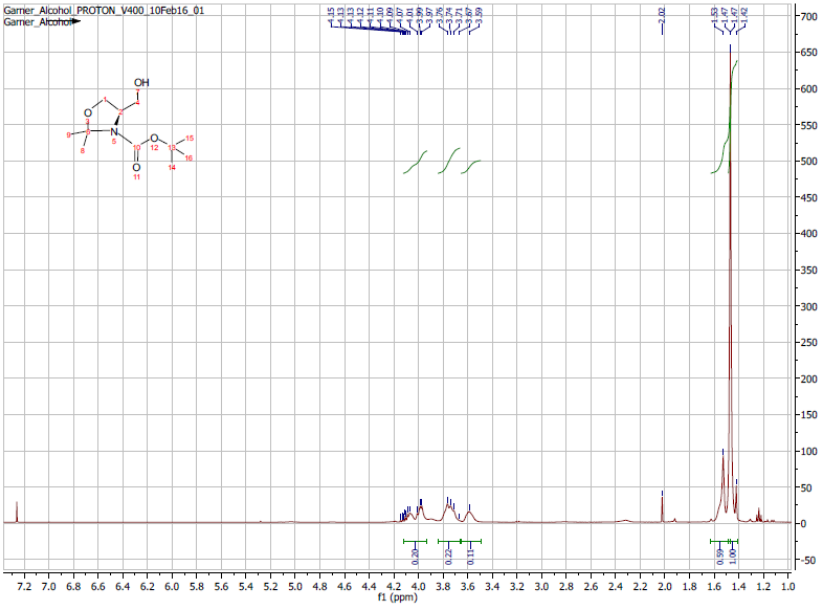

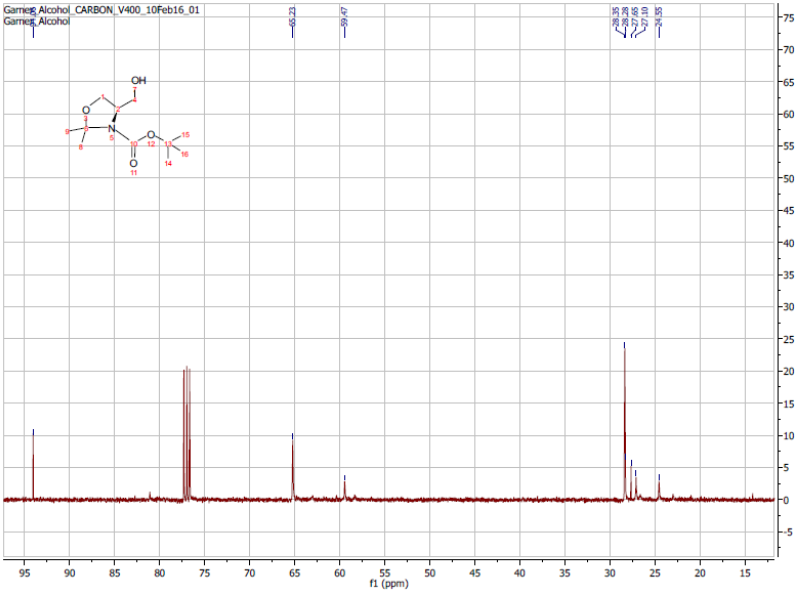

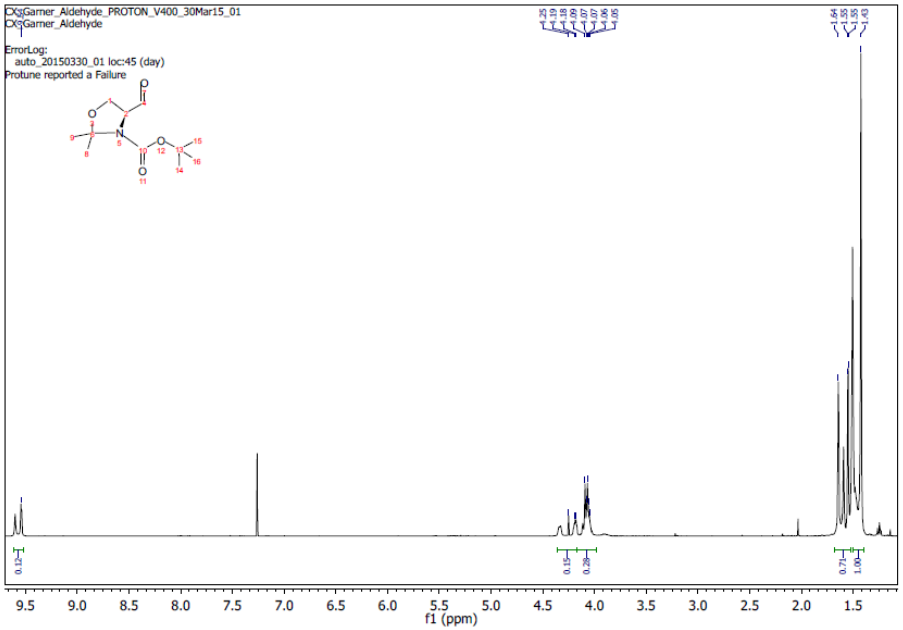
CX:Garner_Aldehyde_PROTON_V400_30Mar15_01
CX:Garner_Aldehyde
ErrorLog:
auto_20150330_01 loc:45 (day)
Protune reported a Failure
f1 (ppm)

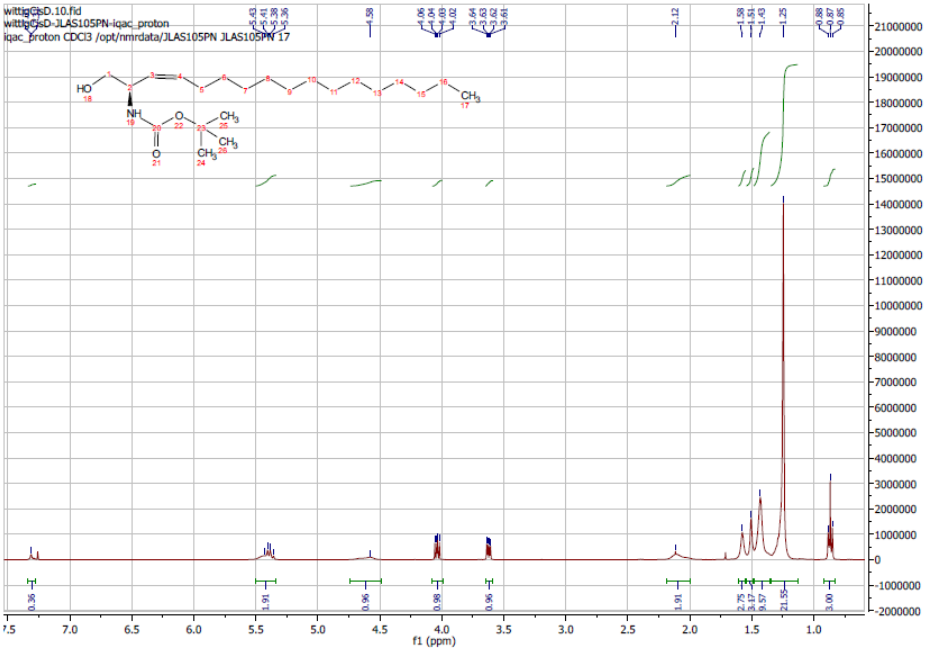
wittigCisD.10.fid
wittigCisD-JLAS105PN-iqac_proton
iqac_proton CDCl3 /opt/nmrdata/JLAS105PN JLAS105PN 17
f1 (ppm)

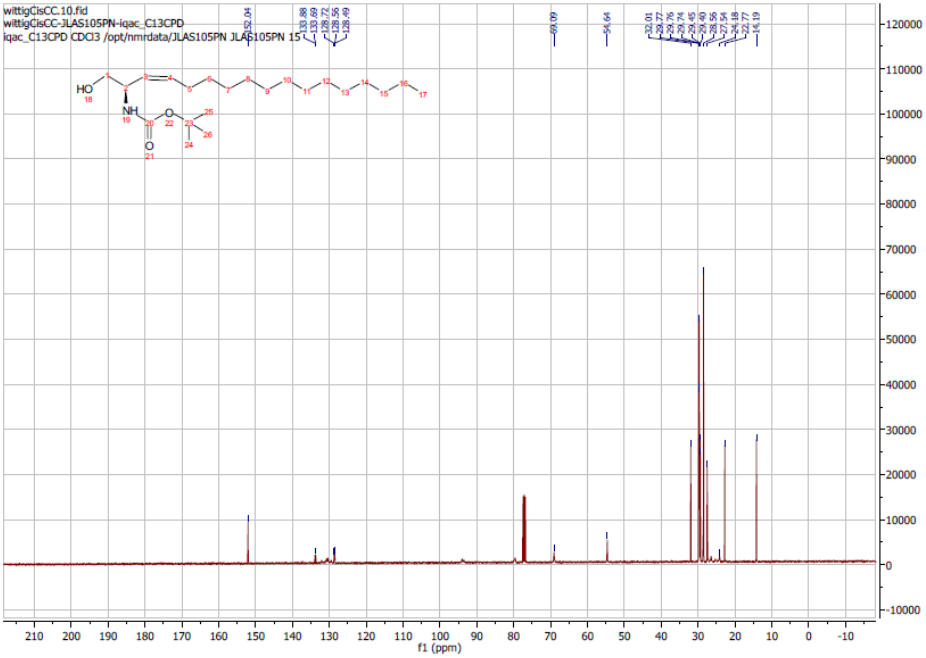
wittigCisCC.10.fid
wittigCisCC-JLAS105PN-iqac_C13CPD
iqac_C13CPD CDCl3 /opt/nmrdata/JLAS105PN JLAS105PN 15
f1 (ppm)

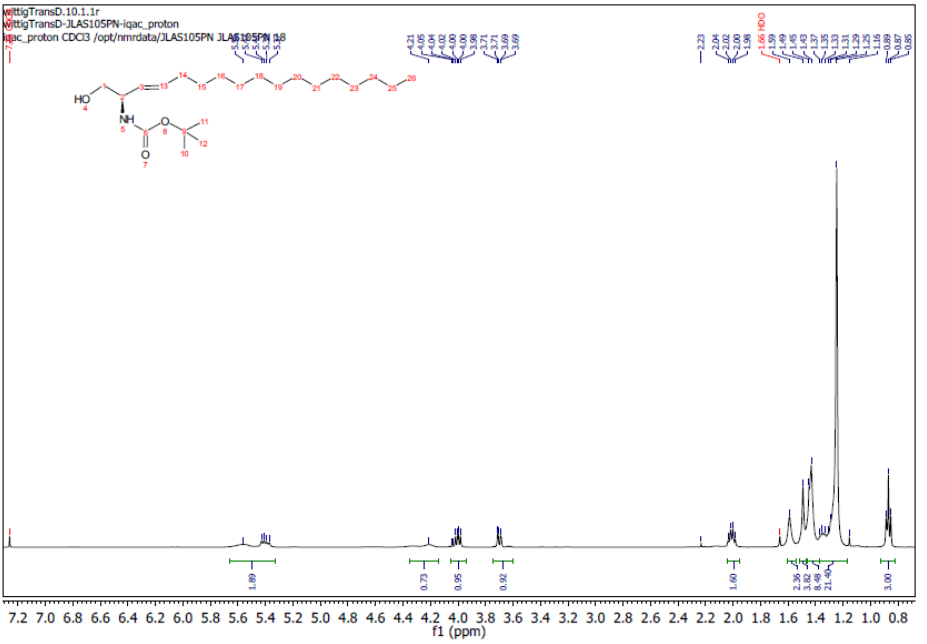
wittigTransD.10.1.1r
wittigTransD-JLAS105PN-iqac_proton
iqac_proton CDCl3 /opt/nmrdata/JLAS105PN JLAS105PN 18
f1 (ppm)

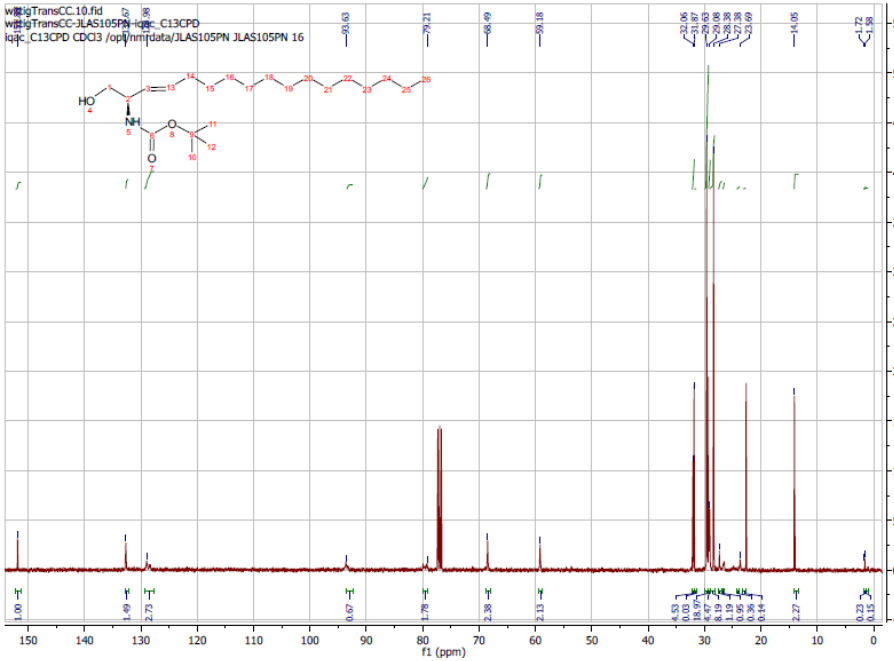
wtligTransCC.10.fid
wtligTransCC-JLAS105PN-iqac_C13CPD
iqac_C13CPD CDCl3 /opt/nmrdata/JLAS105PN JLAS105PN 16
f1 (ppm)

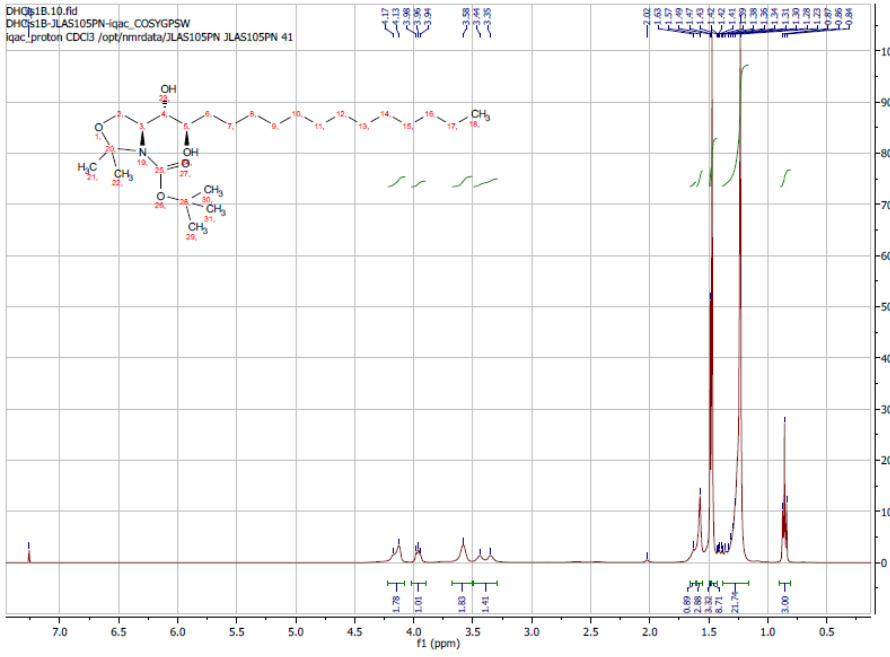
DHQs1B.10.fid
DHQs1B-JLAS105PN-iqac_COSYGPSW
iqac_proton CDCl3 /opt/nmrdata/JLAS105PN JLAS105PN 41
f1 (ppm)

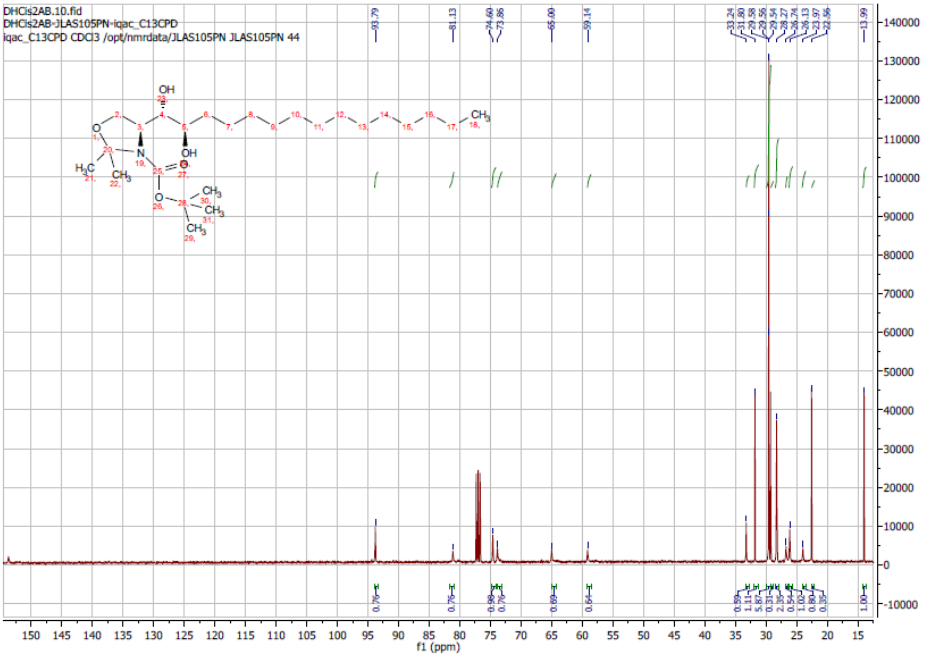
DHCis2AB.10.fid
DHCis2AB-JLAS105PN-iqac_C13CPD
iqac_C13CPD CDCl3 /opt/nmrdata/JLAS105PN JLAS105PN 44
f1 (ppm)

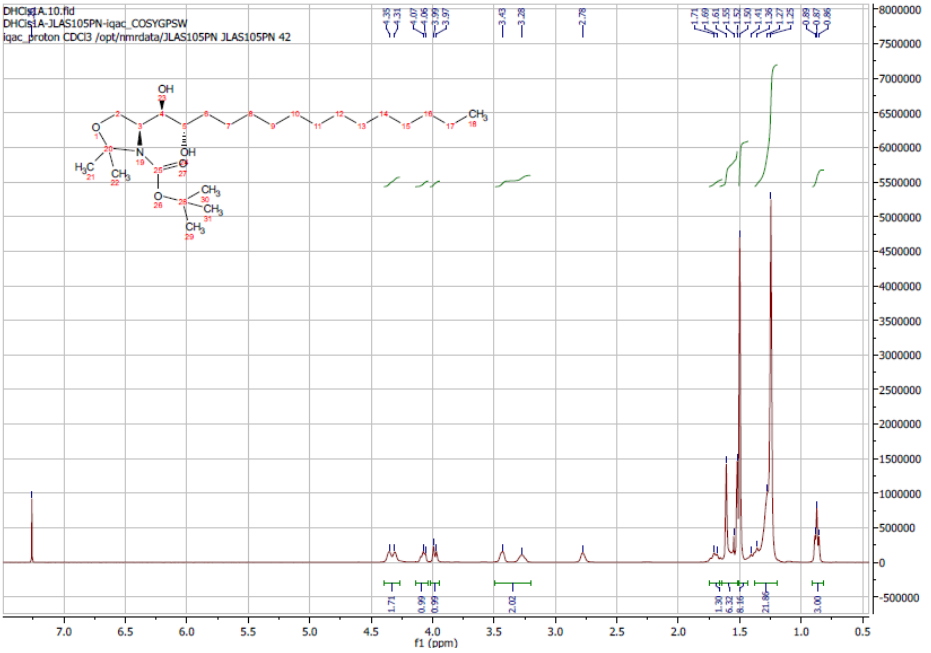
DHCis1A.10.fid
DHCis1A-JLAS105PN-iqac_COSYGPSW
iqac_proton CDCl3 /opt/nmrdata/JLAS105PN JLAS105PN 42
f1 (ppm)

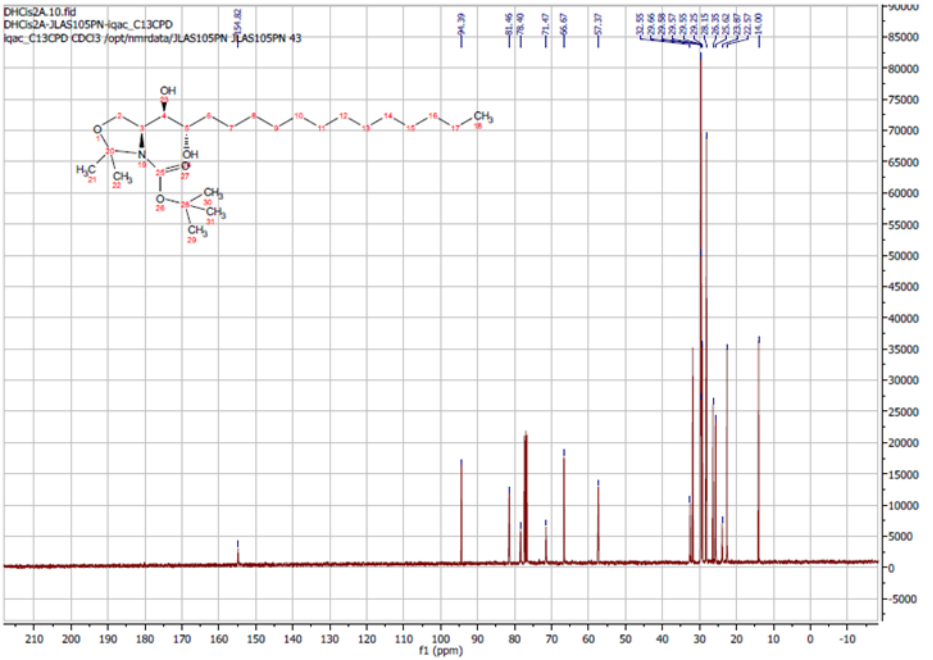
DHCis2A.10.fid
DHCis2A-JLAS105PN-iqac_C13CPD
iqac_C13CPD CDCl3 /opt/nmrdata/JLAS105PN JLAS105PN 43
f1 (ppm)

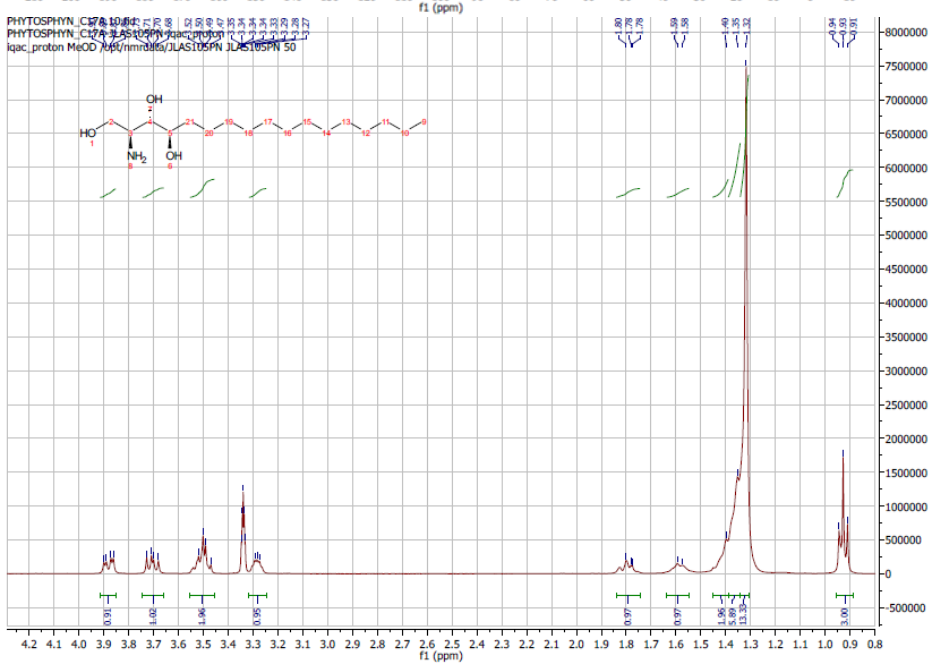
PHYTOSPHYN_C17A-10.fid
PHYTOSPHYN_C17A-JLAS105PN-iqac_proton
iqac_proton MeOD /opt/nmrdata/JLAS105PN JLAS105PN 50
f1 (ppm)

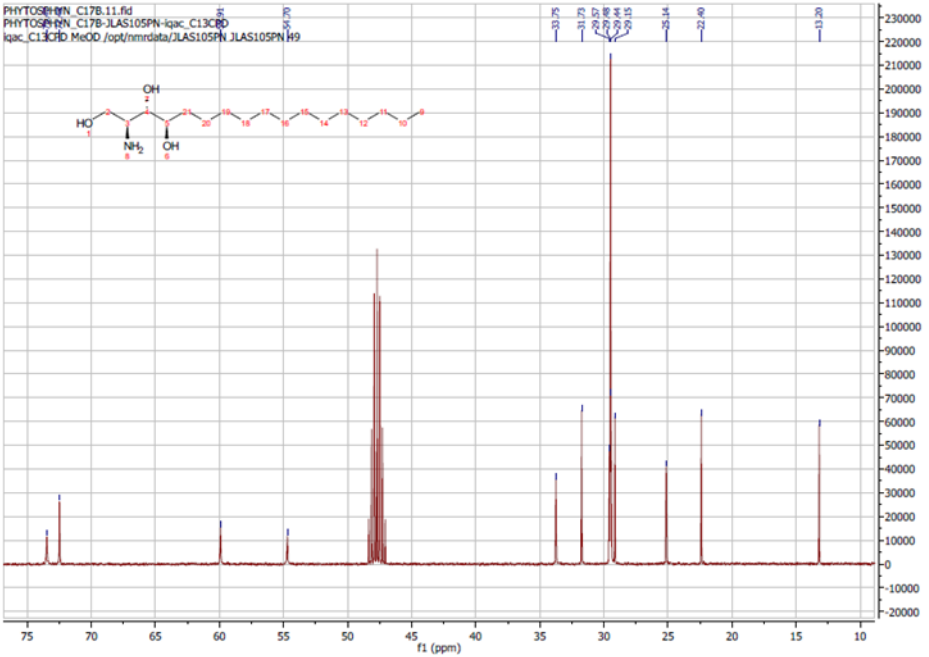
PHYTOSPHYN_C17B.11.fid
PHYTOSPHYN_C17B-JLAS105PN-iqac_C13CPD
iqac_C13CPD MeOD /opt/nmrdata/JLAS105PN JLAS105PN H9
OH
HO
NH2
OH
f1 (ppm)

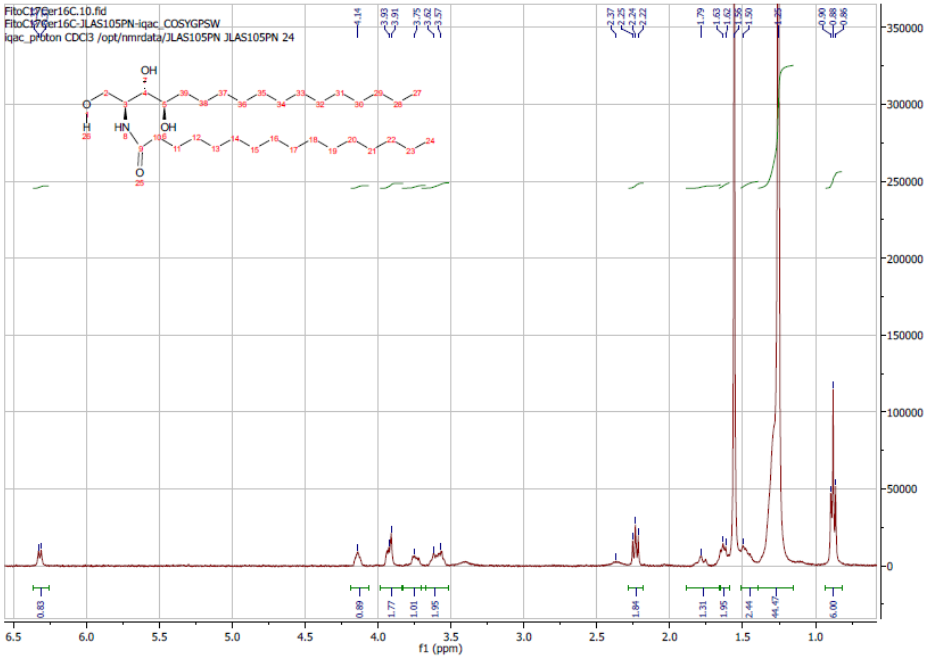
FitoC17Cer16C.10.fid
FitoC17Cer16C-JLAS105PN-iqac_COSYGPSW
iqac_proton CDCl3 /opt/nmrdata/JLAS105PN JLAS105PN 24
OH
O
H
HN
OH
O
f1 (ppm)

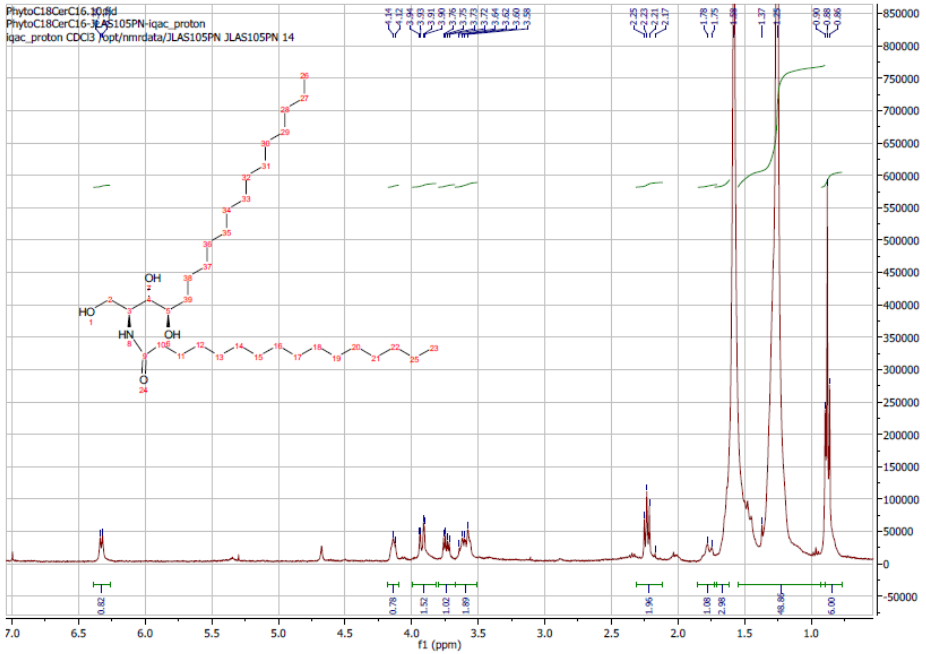
PhytoC18CerC16.10.fid
PhytoC18CerC16-JLAS105PN-iqac_proton
iqac_proton CDCl3 /opt/nmrdata/JLAS105PN JLAS105PN 14
f1 (ppm)